

A0640491

OCD Work Unit No. 3212A

USNRDL-TR-1048

17 January 1966

THREE TESTS OF FIREHOSING TECHNIQUE AND EQUIPMENT  
FOR THE REMOVAL OF FALLOUT FROM ASPHALT STREETS  
AND ROOFING MATERIALS

by

L.L. Wiltshire

W.L. Owen

CLEARINGHOUSE FOR FEDERAL SCIENTIFIC AND TECHNICAL INFORMATION	
Hardcopy	Microfiche
\$3.00	0.75 78 56
ARCHIVE COPY	

D D C  
RECEIVED  
OCT 21 1966  
RECEIVED  
C

U.S. NAVAL RADIOLOGICAL  
DEFENSE LABORATORY

SAN FRANCISCO • CALIFORNIA • 94135

TECHNICAL DEVELOPMENTS BRANCH  
R. R. Soule, Head

CHEMICAL TECHNOLOGY DIVISION  
R. Cole, Head

ADMINISTRATIVE INFORMATION

The work reported was part of a project sponsored by the Office of Civil Defense under Task Order OCD-TO-65-200(22), Work Unit 3212A.

DDC AVAILABILITY NOTICE

Distribution of this document is unlimited.

OCD REVIEW NOTICE

This report has been reviewed in the Office of Civil Defense and approved for publication. Approval does not signify that the contents necessarily reflect the views and policies of the Office of Civil Defense.

ACCESSION FOR	
CFSTI	WHITE SECTION <input checked="" type="checkbox"/>
DDC	BUFF SECTION <input type="checkbox"/>
UNANNOUNCED	<input type="checkbox"/>
JUSTIFICATION	<i>Per statement on Doc</i>
BY <i>Ln</i>	
DISTRIBUTION/AVAILABILITY CODES	
DIST.	AVAIL. and/or SPECIAL
<i>1</i>	

*Eugene P. Cooper*

Eugene P. Cooper  
Technical Director

*D. C. Campbell*

D. C. Campbell, CAPT USN  
Commanding Officer and Director

PAGES \_\_\_\_\_  
ARE  
MISSING  
IN  
ORIGINAL  
DOCUMENT

## SUMMARY

### PROBLEM

Previous reclamation tests of the removal of fallout simulant by firehosing still left several areas requiring further study. First, the latest tests on asphalt streets (in 1963) were not conducted at a large enough scale to either reveal certain important operational effects or to provide exposure-rate history data for deriving  $RN_2$  factors. Second, results from earlier tests indicated that the NRDL experimental flare nozzle showed considerable promise for the reclamation of paved surfaces - as well as roofs. However, data from preliminary test runs on pavement were extremely limited and sketchy. Third, all meaningful roof data had been obtained from only two types of surfaces - tar and gravel and composition shingles. A need existed for studying other materials and for measuring the effects of simulant particle size on firehosing removal effectiveness. In order to meet these requirements a three phase experimental operation was initiated.

### FINDINGS

Three separate experiments were performed at different scales of operation. In all cases, sand tagged with radionuclide  $La^{140}$  was dispersed over the test surfaces to simulate fallout conditions. The scope of the test is tabulated below in terms of the mass loadings used.

Scale of Test	Test Surface	Nozzle Type	Nominal Mass Loading ( $g/ft^2$ )	
			Particle Size Range	
			88-177 $\mu$	300-600 $\mu$
Engineering	Pavement	Flare	5, 25, & 100	5 & 25
Full	Pavement	Fire	25 & 100	5 & 25
Limited	Roofs	Flare	12, 25, 50, & 100	5 & 25
Engineering		and Fire	12, 25, 50, & 100	5 & 25

The findings are as follows:

In general, it may be concluded for both asphalt pavements and roofing materials that:

1. Effectiveness of reclamation by firehosing improves as surface roughness decreases.

2. Larger (300-600  $\mu$ ) particle sizes are more easily removed than the smaller (88-177  $\mu$ ) particle sizes.

3. Removal effectiveness improves with effort, but the residual mass is not significantly reduced after the second pass.

4. The effect of mass loading upon firehosing effectiveness is not predictable because it varies with surface roughness, particle size and nozzle design.

During the engineering-scale tests on asphalt, the flare nozzle failed to exhibit a reclamation performance that was consistently superior to the standard fire nozzle for a significant number of the combinations of mass loading and particle size tested.

The full-scale tests on asphalt showed that operational factors prevent the reclamation effectiveness from ever equaling that achieved at an engineering scale - no matter how much effort is expended. From the exposure rate histories it was found that the exposure reduction factor ( $RN_2$ ) for either the nozzle man or the vehicle operator is not significantly influenced by pavement surface roughness, fallout particle size or mass loading.

The roof firehosing tests demonstrated the superiority of the flare nozzle as a reclamation tool. Fiberglass showed great potential as a durable, easy-to-clean roofing material.

## CONTENTS

ABSTRACT. . . . .	1
SUMMARY . . . . .	11
SECTION I INTRODUCTION. . . . .	1
1.1 Background and History. . . . .	1
1.2 Objectives. . . . .	2
1.3 Experimental Approach and Scope . . . . .	3
SECTION II EXPERIMENTAL PREPARATION AND PROCEDURES . . . . .	5
2.1 Description of Test Sites . . . . .	5
2.2 Firehosing Equipment. . . . .	7
2.3 Simulant Production and Dispersal . . . . .	9
2.4 Radiation Instrumentation . . . . .	9
2.5 Test Procedures . . . . .	10
2.5.1 General Sequence of Operation. . . . .	10
2.5.2 Firehosing Pavement. . . . .	10
2.5.3 Firehosing Roofing Materials . . . . .	12
2.5.4 Procedure. . . . .	15
SECTION III RESULTS AND DISCUSSION. . . . .	16
3.1 Testing the Flare Nozzle on Asphalt Pavement. . . . .	16
3.2 Full-Scale Recovery of Asphalt Pavement by Firehosing . . . . .	17
3.2.1 Removal Effectiveness. . . . .	17
3.2.2 Recovery Exposure. . . . .	20
3.3 Firehosing of Roofing Materials . . . . .	27
3.3.1 Effects of Nozzle Design and Roofing Material. . . . .	27
3.3.2 Mass Loading and Particle Size Effects . . . . .	28
SECTION IV CONCLUSIONS . . . . .	39
SECTION V RECOMMENDATIONS . . . . .	40
REFERENCES . . . . .	41
APPENDIX A REDUCED TEST DATA . . . . .	42
TABLES	
1.1 Basic Conditions of Tests . . . . .	3
3.1 Recovery Exposure-Reduction Factor, $RN_2$ , for Firehosing Crews- Full Scale Tests, Asphalt Pavement Test Area: 8,960 ft <sup>2</sup> (32 x 280 ft) . . . . .	26

SUMMARY OF RESEARCH REPORT

THREE TESTS OF FIREHOSING TECHNIQUE AND EQUIPMENT FOR THE REMOVAL OF  
FALLOUT FROM ASPHALT STREETS AND ROOFING MATERIALS.

USNRDL-TR-1048, dated 17 January 1966 by L. L. Wiltshire and W. L. Owen.

## PURPOSE AND OBJECTIVES

This report describes three separate reclamation experiments that employed firehosing as the fallout removal method. Two of the firehosing experiments were on asphalt streets and conclude the test series started in 1963. The third experiment involved the reclamation of roofing materials and is a renewal of earlier investigations conducted by this laboratory at San Bruno in 1952 and again at Camp Stoneman in 1956 and 1958.

The work performed in 1963 studied the effects of fallout particle size, mass loading, effort expended and removal rate upon the performance of firehosing on contaminated asphalt streets. Although complete in themselves the tests were not conducted at a large enough scale to either fully observe and document operational effects or to obtain the measurements needed for determining exposure reduction factors -  $RN_2$  values.

Results from tests at Stoneman II demonstrated the advantages of an experimental flare nozzle which proved to be as effective as the standard fire nozzle on roofs. More important, the flare nozzle required about 25 % less water per square foot of roof surface cleaned and was less fatiguing to manipulate than the fire nozzle. These two advantages made the flare nozzle worth considering as a tool for the reclamation of paved areas.

Although a number of firehosing tests have been performed on roofs, they have been confined largely to only two types of surface - tar and gravel and composition shingles. In addition, these tests were not designed to determine the influence of particle size upon firehosing effectiveness. Thus, knowledge of roof reclamation needed updating in order to attain a status comparable to that of pavement reclamation.

In the interest of conserving time and making the most of the available equipment and supplies, a three-phase experimental operation was planned. Each phase was designed to satisfy one of the aforementioned requirements.

The objectives of the three phases were as follows:

Phase 1. To conduct engineering-scale tests of the NRDI flare nozzle on asphalt pavement for comparison with previous tests with standard fire nozzle.

Phase 2. To observe the operational problems and to record the exposure rate histories of reclamation crews during the full-scale firehosing tests on asphalt pavement.



Phase 3. To compare the cleaning effectiveness of the fire nozzle and the flare nozzle on selected roofing materials at a limited engineering scale.

The effects of mass loading and particle size were studied in connection with each of the three phases.

#### SCOPE

The three separate experiments were conducted at different scales of operation. The scope of the tests is tabulated below in terms of the mass loading used.

Scale of Test	Test Surface	Nozzle Type	Nominal Mass Loading (g/ft <sup>2</sup> )	
			Particle Size Range	
			88-177 $\mu$	300-600 $\mu$
Engineering	Pavement	Flare	5,25, & 100	5 & 25
Full	Pavement	Fire	25 & 100	5 & 25
Limited	Roofs	Flare	12,25,50, & 100	5 & 25
Engineering		and Fire	12,25,50, & 100	5 & 25

The three scales of experimentation indicated in the table are defined below:

a. Engineering Scale - testing a portion of a target surface that is less than 2000 ft<sup>2</sup> but still large enough to permit the realistic application of full-sized reclamation equipment. In this case the test area comprised a short section of street included between the center line and one curb. This permitted direct comparison with previous engineering-scale tests.

b. Full Scale - testing a complete target component sufficiently greater than 2000 ft<sup>2</sup> to obtain operational information including estimates of recovery crew exposure. The full curb-to-curb width of a street extending the equivalent of one city block was used.

c. Limited Engineering Scale - similar to Engineering Scale except that the test surface is limited to 500 ft<sup>2</sup> or less. Only a fraction of the surfaces for the roof tests was instrumented, since it was not feasible to construct entire roof sections of each material tested.

## FINDINGS

In comparing the effects of nozzle design on firehosing of asphalt pavement, the performance of the flare nozzle surpassed that of the fire nozzle in the removal of the smaller sized particles (88-177  $\mu$ ) and then only at mass loadings significantly less than 100 g/ft<sup>2</sup>. For the remaining test conditions of this phase, the fire nozzle was equal or superior to the flare nozzle.

Dose rate histories of the full scale tests on an asphalt street revealed that the exposure reduction factors (RN<sub>2</sub> values) were 0.20 to 0.27 for nozzle men and 0.07 to 0.11 for the tow truck driver, when restricted to a consideration of just the radiation contributed by the contaminated street.

The superiority of the flare nozzle over the fire nozzle in cleaning roofs was exhibited on all the materials tested. Isolated exceptions occurred, however, when encountering mass loadings of 100 g/ft<sup>2</sup> or particle sizes of 300-600  $\mu$ . This reflected the trend noted earlier in the results of the tests on asphalt.

## CONCLUSIONS

In general, it may be concluded for both asphalt pavements and roofing materials that:

1. Effectiveness of reclamation by firehosing improves as surface roughness decreases.
2. Larger (300-600  $\mu$ ) particle sizes are more easily removed than the smaller (88-177  $\mu$ ) particle sizes.
3. Removal effectiveness improves with effort, but the residual mass is not significantly reduced after the second pass.
4. The effect of mass loading upon firehosing effectiveness is not predictable because it varies with surface roughness, particle size and nozzle design.

During the engineering-scale tests on asphalt, the flare nozzle failed to exhibit a reclamation performance that was consistently superior to the standard fire nozzle for a significant number of the combinations of mass loading and particle size tested.

The full-scale tests on asphalt showed that operational factors prevent the reclamation effectiveness from ever equaling that achieved at an engineering scale - no matter how much effort is expended.

From the exposure rate history it was found that the exposure reduction factor ( $RR_{\lambda}$ ) for either the nozzle man or the vehicle operator is not significantly influenced by pavement surface roughness, fallout particle size or mass loading.

The roof firehosing tests demonstrated the superiority of the flare nozzle as a reclamation tool. Fiberglass showed great potential as a durable, easy-to-clean roofing material.

#### RECOMMENDATIONS

From the results and conclusions obtained in the series of firehosing tests, the following recommendations are made.

1. Investigate feasibility of manufacture and distribution of NRDL flare nozzles to recoverable communities and facilities located in potential fallout areas.

2. If (1) is feasible, employ the NRDL flare nozzle on roofs and in confined paved areas where it is not possible to take advantage of the long reach of the water stream characteristic of fire nozzles.

3. Consider the use of smoother surfaces, such as fiberglass-epoxy, for roofs on vital structures that are likely to require reclamation soon after being contaminated by fallout.

4. Conduct tests on roofing materials at a larger and more realistic scale, or find a suitable method for making operational adjustments to the limited-scale test results. Include the technique of lobbing nozzled water streams from ground level as part of these tests.

A.1	Engineering-Scale Performance Test Results for Flare Nozzle on Rough Asphalt Pavement . . . . .	43
A.2	Engineering-Scale Performance Test Results for Fire Nozzle on Rough Asphalt Pavement (Extracted from 1963 firehosing test results) . . . . .	44
A.3	Full Scale Performance Test Results for Standard Fire Nozzle on Smooth Asphalt Pavement. . . . .	45
A.4	Full Scale Performance Test Results for Standard Fire Nozzle on Rough Asphalt Pavement . . . . .	46
A.5	Limited Engineering Scale Performance Test Results for Fire Nozzle on Roofing Materials Particle Size Range 88-177 $\mu$ ; Nominal Mass Loading 12.0 g/ft <sup>2</sup> . . . . .	47
A.6	Limited Engineering Scale Performance Test Results for Fire Nozzle on Roofing Materials Particle Size Range 88-177 $\mu$ ; Nominal Mass Loading 25.0 g/ft <sup>2</sup> . . . . .	48
A.7	Limited Engineering Scale Performance Test Results for Fire Nozzle on Roofing Materials Particle Size Range 88-177 $\mu$ ; Nominal Mass Loading 50.0 g/ft <sup>2</sup> . . . . .	49
A.8	Limited Engineering Scale Performance Test Results for Fire Nozzle on Roofing Materials Particle Size Range 88-177 $\mu$ ; Nominal Mass Loading 100.0 g/ft <sup>2</sup> . . . . .	50
A.9	Limited Engineering Scale Performance Test Results for Fire Nozzle on Roofing Materials Particle Size Range 300-600 $\mu$ ; Nominal Mass Loading 5.0 g/ft <sup>2</sup> . . . . .	51
A.10	Limited Engineering Scale Performance Test Results for Fire Nozzle on Roofing Materials Particle Size Range 300-600 $\mu$ ; Nominal Mass Loading 25.0 g/ft <sup>2</sup> . . . . .	52
A.11	Limited Engineering Scale Performance Test Results for Flare Nozzle on Roofing Materials Particle Size Range 88-177 $\mu$ ; Nominal Mass Loading 12.0 g/ft <sup>2</sup> . . . . .	53
A.12	Limited Engineering Scale Performance Test Results for Flare Nozzle on Roofing Materials Particle Size Range 88-177 $\mu$ ; Nominal Mass Loading 25.0 g/ft <sup>2</sup> . . . . .	54
A.13	Limited Engineering Scale Performance Test Results for Flare Nozzle on Roofing Materials Particle Size Range 88-177 $\mu$ ; Nominal Mass Loading 50.0 g/ft <sup>2</sup> . . . . .	55
A.14	Limited Engineering Scale Performance Test Results for Flare Nozzle on Roofing Materials Particle Size Range 88-177 $\mu$ ; Nominal Mass Loading 100.0 g/ft <sup>2</sup> . . . . .	56
A.15	Limited Engineering Scale Performance Test Results for Flare Nozzle on Roofing Materials Particle Size Range 300-600 $\mu$ ; Nominal Mass Loading 5.0 g/ft <sup>2</sup> . . . . .	57
A.16	Limited Engineering Scale Performance Test Results for Flare Nozzle on Roofing Materials Particle Size Range 300-600 $\mu$ ; Nominal Mass Loading 25.0 g/ft <sup>2</sup> . . . . .	58

## FIGURES

2.1	Roof Mock-up Showing 4 x 8-ft Panel of Composition Shingles in Place for Testing. . . . .	6
2.2	NRDL Experimental Flare Nozzle, Showing Recessed Elliptical Orifice. . . . .	8
2.3	Layout of Asphalt Test Area for Engineering-Scale Tests of Flare Nozzle, Showing Survey Stations. . . . .	11
2.4	Layout of Asphalt Test Area for Full-Scale Test of Fire Nozzle, Showing Survey Stations. . . . .	11
2.5	Full-Scale Firehosing - Double Crew Procedure, Utilizing Vehicle for Dragging Heavy 2-1/2-in. Firehose. . . . .	13
2.6	Collection of Displaced Simulant Near Mid Point of Curb During the 1st Pass of the 100 g/ft <sup>2</sup> Mass Loading Test . . .	14
3.1	Effects of Nozzle Design and Mass Loading on the Reclamation of Asphalt Pavement for Two Particle Size Ranges, Engineering Scale; 88-177μ, Rough Texture. . . . .	18
3.2	Effects of Nozzle Design and Mass Loading on the Reclamation of Asphalt Pavement for Two Particle Size Ranges, Engineering Scale; 300-600μ, Rough Texture . . . . .	18
3.3	Effects of Mass Loading and Particle Size Range on Full Scale Reclamation of an Asphalt Street for Two Surface Textures - Smooth Texture . . . . .	19
3.4	Effects of Mass Loading and Particle Size Range on Full Scale Reclamation of an Asphalt Street for Two Surface Textures - Rough Texture. . . . .	19
3.5	Exposure Rate History for Recovery of Asphalt Pavement by Firehosing; Full Scale Test, 300-600μ, 4.4 g/ft <sup>2</sup> . . . . .	22
3.6	Exposure Rate History for Recovery of Asphalt Pavement by Firehosing; Full Scale Test, 300-600μ, 24.24 g/ft <sup>2</sup> . . . . .	23
3.7	Exposure Rate History for Recovery of Asphalt Pavement by Firehosing; Full Scale Test, 88-177μ, 25.02 g/ft <sup>2</sup> . . . . .	24
3.8	Exposure Rate History for Recovery of Asphalt Pavement by Firehosing; Full Scale Test, 88-177μ, 92.4 g/ft <sup>2</sup> . . . . .	25
3.9	Comparison of Nozzle Design and Roofing Material Effects for Particle Size Range 88-177μ at a Mass Loading of 12.0 g/ft <sup>2</sup> , Composition Shingles/Asphaltum . . . . .	30
3.10	Comparison of Nozzle Design and Roofing Material Effects for Particle Size Range 88-177μ at a Mass Loading of 12.0 g/ft <sup>2</sup> , Fiberglass/Galvanized Sheeting. . . . .	30
3.11	Comparison of Nozzle Design and Roofing Material Effects for Particle Size Range 88-177μ at a Mass Loading of 25.0 g/ft <sup>2</sup> , Composition Shingles/Asphaltum. . . . .	31
3.12	Comparison of Nozzle Design and Roofing Material Effects for Particle Size Range 88-177μ at a Mass Loading of 25.0 g/ft <sup>2</sup> , Fiberglass/Galvanized Sheeting. . . . .	31

3.13	Comparison of Nozzle Design and Roofing Material Effects for Particle Size Range 88-177 $\mu$ at a Mass Loading of 50.0 g/ft <sup>2</sup> , Composition Shingles/Asphaltum. . . . .	32
3.14	Comparison of Nozzle Design and Roofing Material Effects for Particle Size Range 88-177 $\mu$ at a Mass Loading of 50.0 g/ft <sup>2</sup> , Fiberglass/Galvanized Sheeting. . . . .	32
3.15	Comparison of Nozzle Design and Roofing Material Effects for Particle Size Range 88-177 $\mu$ at a Mass Loading of 100.0 g/ft <sup>2</sup> , Composition Shingles/Asphaltum . . . . .	33
3.16	Comparison of Nozzle Design and Roofing Material Effects for Particle Size Range 88-177 $\mu$ at a Mass Loading of 100.0 g/ft <sup>2</sup> , Fiberglass/Galvanized Sheeting . . . . .	33
3.17	Comparison of Nozzle Design and Roofing Material Effects for Particle Size Range 300-600 $\mu$ at a Mass Loading of 5.0 g/ft <sup>2</sup> , Composition Shingles/Asphaltum. . . . .	34
3.18	Comparison of Nozzle Design and Roofing Material Effects for Particle Size Range 300-600 $\mu$ at a Mass Loading of 5.0 g/ft <sup>2</sup> , Fiberglass/Galvanized Sheeting. . . . .	34
3.19	Comparison of Nozzle Design and Roofing Material Effects for Particle Size Range 300-600 $\mu$ at a Mass Loading of 25.0 g/ft <sup>2</sup> , Composition Shingles/Asphaltum. . . . .	35
3.20	Comparison of Nozzle Design and Roofing Material Effects for Particle Size Range 300-600 $\mu$ at a Mass Loading of 25.0 g/ft <sup>2</sup> , Fiberglass/Galvanized Sheeting. . . . .	35
3.21	Comparison of the Effects of Mass Loading and Particle Size Range on Hosing Performance for Two Nozzle Designs on Fiberglass Roofing Material - Fire Nozzle. . . . .	36
3.22	Comparison of the Effects of Mass Loading and Particle Size Range on Hosing Performance for Two Nozzle Designs on Fiberglass Roofing Material - Flare Nozzle . . . . .	36
3.23	The Effects of Mass Loading and Particle Size Range on Hosing Performance of the Fire Nozzle on Corrugated Metal Roofing Material - Fire Nozzle. . . . .	37
3.24	The Effects of Mass Loading and Particle Size Range on Hosing Performance of the Fire Nozzle on Corrugated Metal Roofing Material - Flare Nozzle . . . . .	37
3.25	Comparison of the Effects of Mass Loading and Particle Size Range on Hosing Performance of Two Nozzle Designs on Composition Shingle Roofing Material - Fire Nozzle . . . . .	38
3.26	Comparison of the Effects of Mass Loading and Particle Size Range on Hosing Performance of Two Nozzle Designs on Composition Shingle Roofing Material - Flare Nozzle. . . . .	38

## SECTION I

### INTRODUCTION

This report describes three separate reclamation experiments that employed firehosing as the fallout removal method. Two of the firehosing experiments were on asphalt streets and conclude the test series started in 1963.\* The third experiment involved the reclamation of roofing materials and is a renewal of earlier investigations conducted by this laboratory at San Bruno in 1952<sup>1</sup> and again at Camp Stoneman in 1956<sup>2</sup> and 1958.<sup>3</sup>

#### 1.1 BACKGROUND AND HISTORY

The work performed in 1963\* studied the effects of fallout particle size, mass loading, effort expended, and removal rate upon the performance of firehosing on contaminated asphalt streets. The tests were conducted at an engineering scale; i.e., the test surface was limited to a short section of street included between the center line and one curb. Although complete in themselves, these tests did not reveal the adverse operational effects\*\* that could accompany a full-scale test performed from curb to curb and 200 or 300 ft down the length of a typical street. Because of the limited scale, it was not possible to obtain data necessary for deriving exposure reduction factors ( $RN_2$  values) for the firehosing team.

---

\* The results of the 1963 firehosing test series are to be reported in a forthcoming USNRDL TR by the authors entitled "Removal of Simulated Fallout From Asphalt Streets by Firehosing Techniques."

\*\*Increased surface area can lead to excessive build-up of accumulated contaminant (see Section 2.5.1 b). Increases in the number of reclamation personnel usually reduce operational efficiency.

Results from tests at Stoneman II<sup>3</sup> demonstrated the advantages of an experimental flare nozzle used in firehosing roofs. This nozzle provided a flat, fan-shaped stream which was ideal for working at close range. It proved to be as effective as the standard fire nozzle. More important, the flare nozzle required about 25 % less water per square foot of roof surface cleaned and was less fatiguing to manipulate than the fire nozzle. These two advantages made the flare nozzle worth considering as a tool for the reclamation of paved areas.

Although a number of firehosing tests have been performed on roofs, they have been confined largely to only two types of surface - tar and gravel and composition shingles. In addition, these tests were not designed to determine the influence of particle size upon firehosing effectiveness. Thus, knowledge of roof reclamation needed updating in order to attain a status comparable to that of pavement reclamation.

In the interest of conserving time and making the most of the available equipment and supplies, a three-phase experimental operation was planned. Each phase was designed to satisfy one of the aforementioned requirements.

## 1.2 OBJECTIVES

The objectives of the three phases were as follows:

Phase 1. To conduct engineering-scale tests of the NRDL flare nozzle on asphalt pavement for comparison with previous tests with a standard fire nozzle.

Phase 2. To observe the operational problems and to record the exposure rate histories of reclamation crews during the full-scale firehosing tests on asphalt pavement.

Phase 3. To compare the cleaning effectiveness of the fire nozzle and the flare nozzle on selected roofing materials at a limited engineering scale.

The effects of mass loading and particle size were studied in connection with each of the three phases.



### 1.3 EXPERIMENTAL APPROACH AND SCOPE

The three separate experiments were conducted at different scales of operation. The scope of the tests is shown in Table 1.1, in terms of the mass loading used.

TABLE 1.1

Basic Conditions of Tests

Scale of Test	Test Surface	Nozzle Type	Nominal Mass Loading (g/ft <sup>2</sup> ) Particle Size Range	
			88-177 $\mu$	300-600 $\mu$
Engineering	Pavement	Flare	5, 25, & 100	5 & 25
Full	Pavement	Fire	25 & 100	5 & 25
Limited Engineering	Roofs	Flare and Fire	12, 25, 50, & 100	5 & 25
			12, 25, 50, & 100	5 & 25

The three scales of experimentation indicated in Table 1.1 are defined below:

a. Engineering Scale - testing a portion of a target surface that is less than 2000 ft<sup>2</sup> but still large enough to permit the realistic application of full-sized reclamation equipment. In this case the test area comprised a short section of street included between the center line and one curb. This permitted direct comparison with previous engineering-scale tests.

b. Full Scale - testing a complete target component sufficiently greater than 2000 ft<sup>2</sup> to obtain operational information including estimates of recovery crew exposure. The full curb-to-curb width of a street extending the equivalent of one city block was used.

c. Limited Engineering Scale - similar to Engineering Scale except that the test surface is limited to 500 ft<sup>2</sup> or less. Only a fraction of the surfaces for the roof tests was instrumented, since it was not feasible to construct entire roof sections of each material tested. (The roof mock-up used is described in Section II.)

Six of the mass loading and particle size combinations shown in Table 1.1 are within the range of values consistent with Miller's concept of a fallout scaling system.<sup>4</sup> Radiological conditions corresponding to these combinations are given in the following table. These standard exposure rates, weapon yields, and downwind distances were derived from the work of Clark and Cobbin (Ref. 5, App. C), which, in turn, was an extension of Miller's fallout model.

Particle Size Range (μ)	Exposure Rate at One Hour (r/hr)					Kiloton Yield	Miles Down- wind
	Nominal Mass Loadings (g/ft <sup>2</sup> )						
	5	12	24	50	100		
88-177	X	-	12,000	(25,000)	(50,000)	25,000	90
300-600	700	(1,700)	(3,400)	X	X	100	12

Note: Exposure rates shown in parentheses are the result of multiple bursts.

The remaining three combinations, indicated by the X's in the above table, were not derived from Miller's model. They were added arbitrarily to take advantage of open spaces in the weekly schedule.

## SECTION II

### EXPERIMENTAL PREPARATION AND PROCEDURES

#### 2.1 DESCRIPTION OF TEST SITES

Different test sites were used for each test. The flare nozzle was proof-tested on the test strip used in previous firehosing tests, which were of engineering scale. In these tests only the asphalt half of the test strip, from the center line to one curb, was used. The surface was asphaltic concrete, which had an even, coarse-grained texture. The asphalt test section was 14 ft wide and 95 ft long.

The full-scale test on the reclamation of asphalt pavement by firehosing was conducted on a section of street 32 ft wide and 280 ft long. The full width of the street was used from curb to curb. Three-quarters (24 ft) of the street width along one curb was smoothly textured, but the remaining quarter (8 ft along the other curb) was coarse-textured for the entire length of the test section.

The limited engineering-scale tests of the fire and flare nozzles on roofing materials used the roof mock-up shown in Fig. 2.1. This mock-up consisted of a plane 12 ft deep and 16 ft wide, with a slope of 3.5 in./ft. A 4 x 8-ft recess for the various test panels of roofing materials was centered longitudinally in the plane. The surface surrounding the test panel opening was covered with fiberglass in which coarse sand was imbedded to make a safe walkway for test personnel. Sixteen panels (4 x 8 ft) were employed to test the following roofing materials: fiberglass, asphaltum, corrugated metal, and composition shingle.

The fiberglass surface was made by imbedding a single layer of glass fabric in an epoxy resin which formed a permanent bond with the plywood panel. Asphaltum test panels were made by trowelling Lay Kold Walk-top (a mineral-filled, fibrous, bituminous composition) onto plywood. The corrugated metal sheet and the heavy-weight square-tabbed composition shingles were applied to the panels with nails in the conventional manner.



Fig. 2.1 Roof Mock-up Showing 4 x 8-ft panel of Composition Shingles in Place for Testing.

## 2.2 FIREHOSING EQUIPMENT

Two types of nozzle were used in these tests. The standard tapered fire nozzle (1-1/2 in., with a 5/8-in. bore) formed a slender cone-shaped stream of water at nozzle pressures of 60 and 75 psi. The experimental NRDL flare nozzle (1 in., with an elliptical orifice 3/8 x 9/16 in., Fig. 2.2) delivered a flat, fan-shaped stream of water at nozzle pressures of 120 and 160 psi.

In these tests the nozzles were always used with standard firehosing equipment. A fire pump inserted into the system at the fire hydrant delivered water through a 2-1/2-in. fire hose to a wye-gate at the test area. For the engineering and limited-engineering scale tests, one branch of the wye gate supplied water to the nozzle through a 1-1/2-in. fire hose. A by-pass hose connected to the remaining branch and valve assembly at the wye-gate were used to adjust the nozzle pressure and flow rate. For the full scale tests, each branch of the wye gate supplied water to a 1-1/2 in. fire hose, and adjustments to pressure and flow were made at the pump.

The following table summarizes the values of the hydrodynamic parameters characterizing the two nozzles.

Nozzle Type	Test Surface	Nozzle Orifice (in.)	Nozzle Pressure (psi)	Nozzle Thrust (lb)	Flow Rate (gpm)
Standard Fire	Pavement	5/8	75	46	100
	Roofs	5/8	60	37	89
NRDL Flare	Pavement	3/8 x 9/16	160	46	70
	Roofs	3/8 x 9/16	120	36	60

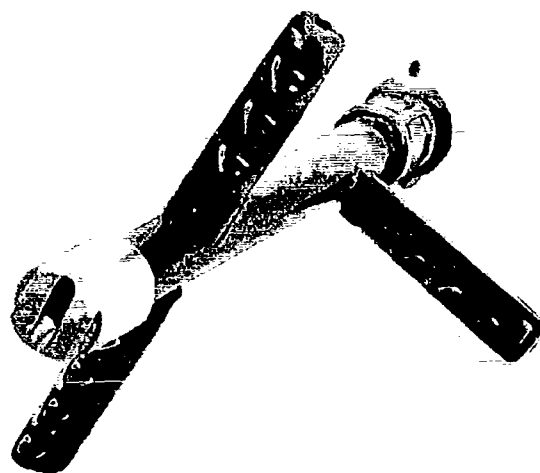


Fig. 2.2 NRDL Experimental Flare Nozzle, Showing  
Recessed Elliptical Orifice.

### 2.3 SIMULANT PRODUCTION AND DISPERSAL

The fallout simulant and dispersing equipment were of the type used in the 1963 tests at Camp Parks (see footnotes on page 1). These tests used fallout simulant in two particle size ranges (88-177  $\mu$  and 300-600  $\mu$ ). The simulant was sieved from commercial sand, tagged with the radionuclide  $\text{La}^{140}$ , and sealed against leaching. For further information on the development of the fallout simulants see Ref. 6.

Uniform mass loadings on all surfaces were achieved by dispersing the simulant over a known area with a calibrated, hand-operated lawn spreader. The average mass loading per square foot was calculated from the actual weight of simulant used in each test.

### 2.4 RADIATION INSTRUMENTATION

The principal instrument for measuring residual mass loading was the mobile, shielded and collimated gamma-detector. This field instrument employs a sodium iodide scintillation crystal, coupled to a photomultiplier tube within a thick lead shield. The detector's physical characteristics are:

- a. Crystal - 1 X 1 in. cylinder approximately 1 meter above the surface.
- b. Lead shield - 4 in. thick with a collimated 1-in. diameter aperture.
- c. Field of view - subtended by a cone having an included angle of  $140^\circ$ .

The standard AN/PDR-27F radiac was used for back-up surveys in case of malfunctioning of the mobile gamma-detector. The radiac also was used to collect the exposure rate history data of the recovery crews.

The 4-pi ionization chamber, a stationary laboratory instrument, was used for simulant production control. Details of this and the above instruments are to be found in Ref. 7.

## 2.5 TEST PROCEDURES

### 2.5.1 General Sequence of Operation

A typical test was carried out in the following sequence. The test area (whether pavement or roof) was thoroughly flushed of all residue from previous tests and then allowed to dry. The residual background radiation level was measured. Fallout simulant at a selected mass loading and particle size range was dispersed over the test area and initial radiation measurements were made. The firehosing operation was performed as detailed later in this section, and the residual radiation was measured. These radiation measurements were repeated after each additional firehosing pass. All surveys of asphalt test areas were made with the two kinds of detectors, the shielded detector and the radiac at the survey stations shown in Figs. 2.3 and 2.4. Roof surfaces were surveyed with the shielded detector only at two stations, one in each half of the test panel.

### 2.5.2 Firehosing Pavement

The previously proven frontal-sweeping hosing technique\* was employed during both phases of the experiments on asphalt paving. Starting at one end of the test strip fire nozzles were played back and forth between the side lines as the firehosing team moved toward the other end. Each test consisted of two or three passes. The visually controlled rate of firehosing was used in these tests. In other words, forward progress was governed by the rate at which the loosened fallout simulant appeared to move down course ahead of the water stream.

#### a. Testing the Flare Nozzle

These tests were performed at an engineering scale on the asphalt test strip. The frontal-sweeping firehosing technique was used. The flare nozzle was operated at a nozzle pressure of 160 psi, from a height of 40 in. and at specified ranges in the interval 5 to 15 ft.

#### b. Full-Scale Firehosing Tests

The full-scale reclamation of an asphalt street by firehosing, with a standard fire nozzle, was an extension of the 1963 engineering-scale tests. The basic frontal-sweeping technique mentioned above was used. The fire nozzle was operated at a nozzle pressure of 75 psi, from a height of 40 in. and at ranges of 20 to 25 ft. For the full width street a two-nozzle double-crew procedure was employed. Two

\* Described in reference given in footnote on page 1.



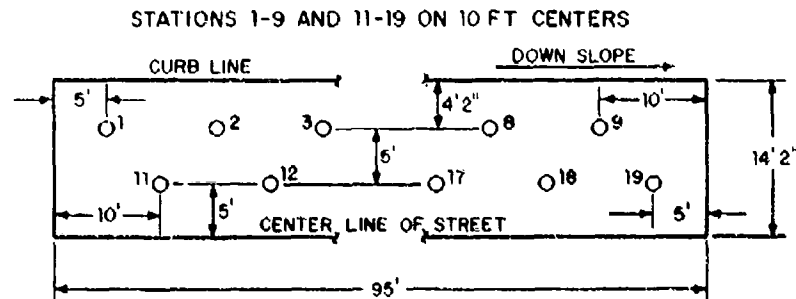


Fig. 2.3 Layout of Asphalt Test Area for Engineering-Scale Tests of Flare Nozzle, Showing Survey Stations.

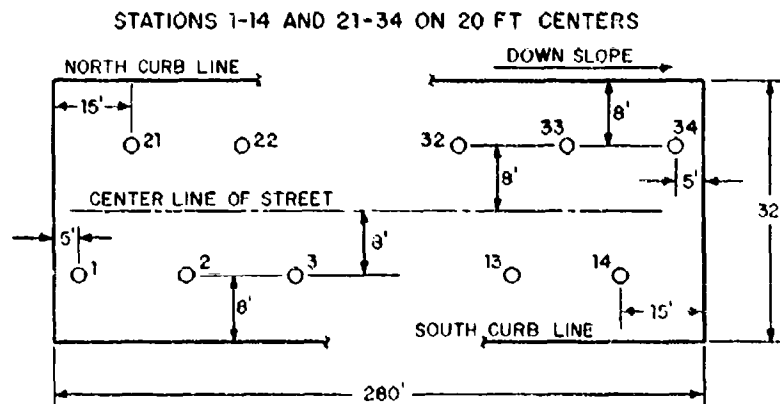


Fig. 2.4 Layout of Asphalt Test Area for Full-Scale Test of Fire Nozzle, Showing Survey Stations.

firehosing teams advanced side by side down the street, cleaning it at the visually controlled rate. A pick-up truck towed the wye-gate and heavy 2-1/2-in. firehose to reduce the number of men required to support the nozzle operators, Fig. 2.5. Three firehosing passes were made in each test. The exposure rate histories of the crew members were collected with radiacs during the first pass only.

When a mass loading of  $100 \text{ g/ft}^2$  was spread, the increased weight of simulant called for a change in firehosing procedure. Because of the accelerated mass build-up of simulant in front of the water streams, the cleaning rate would have been drastically reduced during the latter half of the first pass. Therefore, the firehosing teams deposited the contaminant collected from the first half of the test strip at a point near one curb and midway between the ends of the test strip (see Fig. 2.6). The team then continued hosing the remaining half and pushed the resultant accumulation off the end of the strip. These deposits were shoveled into an end loader and removed to the waste pit prior to the second and third firehosing pass. The latter were performed in the usual manner described earlier in this section.

### 2.5.3 Firehosing Roofing Materials

The firehosing procedure for roofs was a little different from that for pavements. Lower nozzle pressures (fire nozzle, 60 psi; and flare nozzle, 120 psi) were used for the safety of the nozzleman. Shorter stream ranges were used for the fire nozzle. The test procedure sequence was as follows:

- a. The roof mock-up (test plane and roof panel) was flushed of all residue from previous tests and allowed to dry.
- b. The test panel was placed under the shielded detector and the residual background radiation level of the panel was measured. Two 1-min counts were made on each half of the test panel.
- c. The panel was repositioned in the roof plane recess and the entire surface was contaminated with a selected mass loading and particle size range.
- d. The panel was carefully removed, counted under the shielded detector, and repositioned in the test roof plane.
- e. The roof panel and plane assembly were firehosed from the peak to the eaves at the visually controlled rate.
- f. The panel was removed, counted, and repositioned for the next firehosing pass.

Usually three firehosing passes were made. During firehosing operations, only one man (the nozzle operator) was required on the roof. The rest of the team stood by to regulate the water pressure and to handle and survey the test panel.

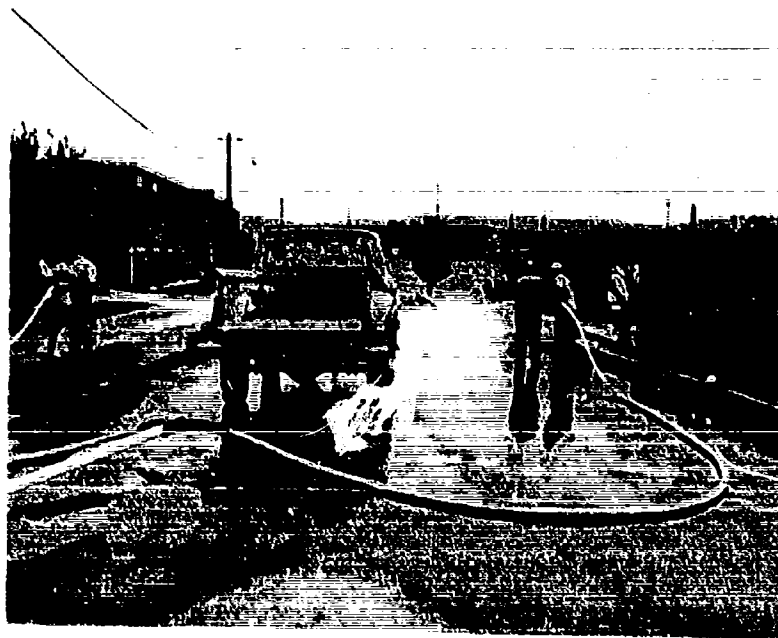


Fig. 2.5 Full-Scale Firehosing - Double Crew Procedure,  
Utilizing Vehicle for Dragging Heavy 2-1/2-in. Firehose.



Fig. 2.6 Collection of Displaced Simulant Near Mid Point of Curb During the 1st Pass of the 100 g/ft<sup>2</sup> Mass Loading Test.

#### 2.5.4 Procedure

Radiation measurements were taken periodically during all test runs to determine background radiation level, initial radiation level, and the residual radiation level after each hosing pass. The mobile detector routine for each instrument pass was as follows:

- a. Instrument response was determined by counting a  $\text{Co}^{60}$  radiation standard in a low background area.
- b. At each survey station two 1-min counts were made and recorded.
- c. The instrument was again checked with the  $\text{Co}^{60}$  standard.

The routine for the 27-F radiac was much simpler. The radiac response was checked with a  $\text{Co}^{60}$  standard before and after each day's tests. The measurements at each survey station were made at 1 meter above the surface.

Time and motion studies were made to obtain cleaning rate, effort, and exposure rate histories for all four full scale recovery tests. The exposure rate histories of the two nozzle men and the tow operator were obtained during the first firehosing pass of each test (see Figs. 3.5-3.8). Exposure rates were taken with a 27-F radiac at one meter above the street surface near the nozzle men and inside the cab at seat level near the tow truck operator. The measurements were made every 30 to 60 sec., and the times were recorded to complete the history.

## SECTION III

### RESULTS AND DISCUSSION

The reduced data from all of the firehosing performance tests are presented in sixteen self-explanatory tables in Appendix A. This information has been condensed from raw data obtained by the shielded gamma-detector surveys and the time and motion studies. The test results are best portrayed by the reclamation performance curves plotted directly from the tabular data. It should be pointed out that while data points are connected by straight lines this does not necessarily indicate the path between any two successive points.

#### 3.1 TESTING THE FLARE NOZZLE ON ASPHALT PAVEMENT

In order to compare performances, the flare nozzle was tested against all the same combinations of particle size and mass loading previously used with the fire nozzle. The reduced test data are compiled in Table A.1. Table A.2 contains results from the 1963 tests (referred to on page 1) for the 1-1/2-in. fire nozzle on asphalt pavement. Figures 3.1 and 3.2 contain ten performance curves grouped according to particle size range. They show the residual mass,  $M$ , as a function of effort,  $E$ , for each test.

A comparison of the current tests with the 1963 results shows that for particle size range 88-177  $\mu$  the flare nozzle was more effective than the fire nozzle at mass loadings less than 100 g/ft<sup>2</sup>. For the same particle size range the fire nozzle was more effective against the heavier mass loading of 100 g/ft<sup>2</sup>. At the larger particle size range of 300-600  $\mu$  the fire nozzle was superior against the 5-g/ft<sup>2</sup> mass loading, but its performance against 25 g/ft<sup>2</sup> was indistinguishable from that of the flare nozzle.

According to the converging behavior of the solid curves in Fig. 3.1, mass loading has little effect on the performance of the fire

nozzle when particle size is small. The curves for the flare nozzle indicate that, in general, high residual mass is associated with high initial mass loading, although curves for the 5 and 25 g/ft<sup>2</sup> mass loadings converge. According to Fig. 3.2 this also appears to be the case for both nozzles when particle size is large. Comparing the fire nozzle curves of Fig. 3.1 and 3.2 it is also apparent that, for mass loadings less than 100 g/ft<sup>2</sup>, the fire nozzle removes the larger particles more readily than the smaller ones. In the case of the flare nozzle, the influence of particle size is not nearly so evident.

### 3.2 FULL-SCALE RECOVERY OF ASPHALT PAVEMENT BY FIREHOSING

Four firehosing tests were conducted at full scale to determine the influence of operational factors on removal effectiveness and to obtain exposure-rate histories of hosing crews.

#### 3.2.1 Removal Effectiveness

The reduced test data are compiled in Tables A.3 and A.4 for smooth and rough surfaces, respectively. They are plotted in eight performance curves (Figs. 3.3 and 3.4) of residual mass,  $M$ , versus effort,  $E$ , for each test.

Both these families of curves are quite similar in that each reflects the finding noted above for mass loading effects. That is, mass loading influences fire nozzle performance only when particle size is large. It is immediately obvious, from comparing the two families of curves, that the smoothly textured asphalt is cleaned more effectively than the rougher surface. A comparison of the residual fractions in Tables A.3 and A.4 shows that these relative effectivenesses differ by factors of 2 or 3. The quickly decreasing slope in all the curves indicates that any gain in effectiveness after two passes does not warrant the added effort.

The relative location of the two pairs of curves plotted for a mass loading of 25 g/ft<sup>2</sup> shows that the larger particles are more easily removed than the smaller ones. This coincides with results of previous wet method tests including firehosing and street flushing.<sup>8</sup>

Probably the most important finding of these tests is disclosed when the engineering-scale and full-scale performances of the fire nozzle are compared for asphalt pavement having rough textured surfaces.

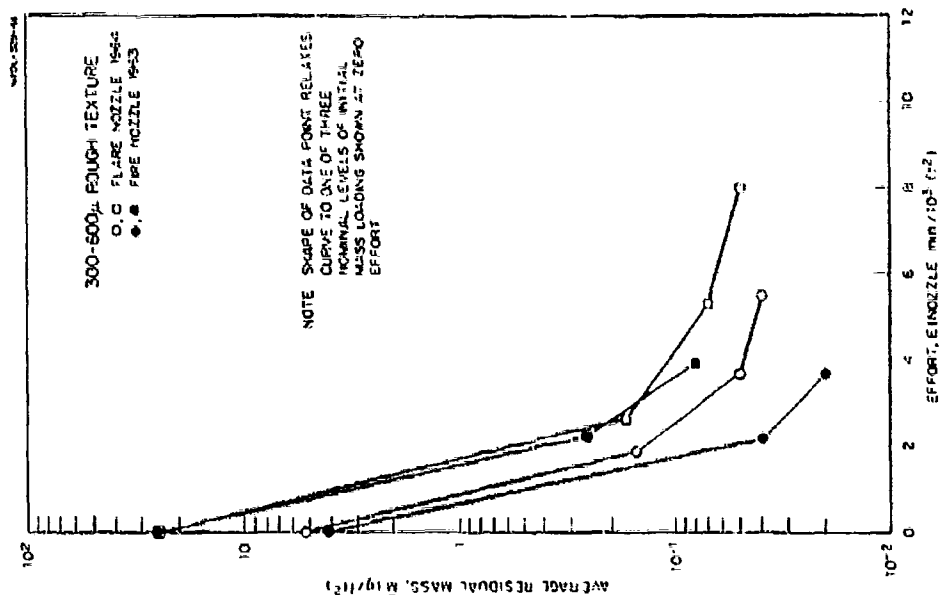


Fig. 3.2

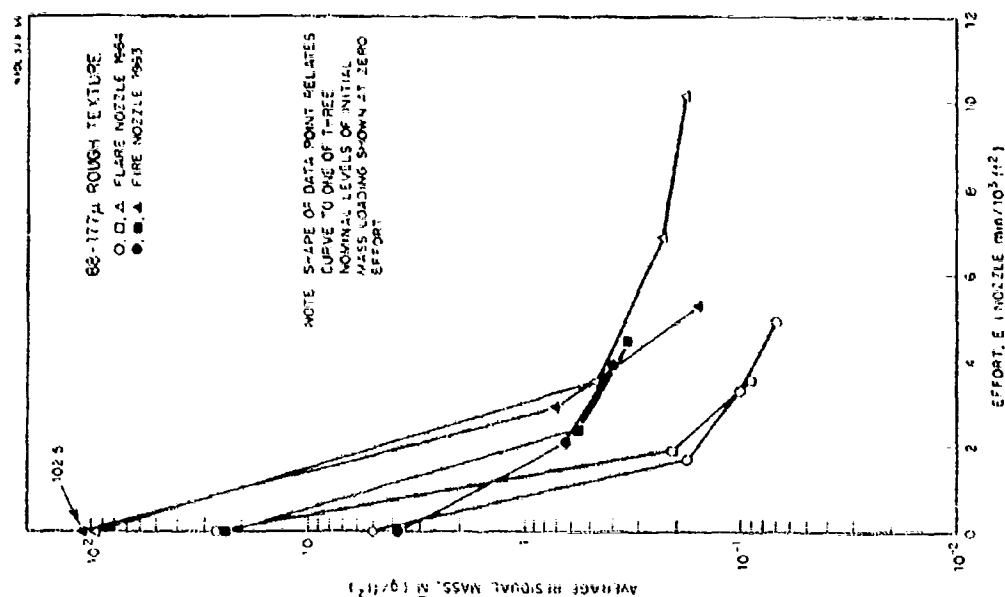


Fig. 3.1

Effects of Nozzle Design and Mass Loading on the Reclamation of Asphalt Pavement for Two Particle Size Ranges, Engineering Scale.



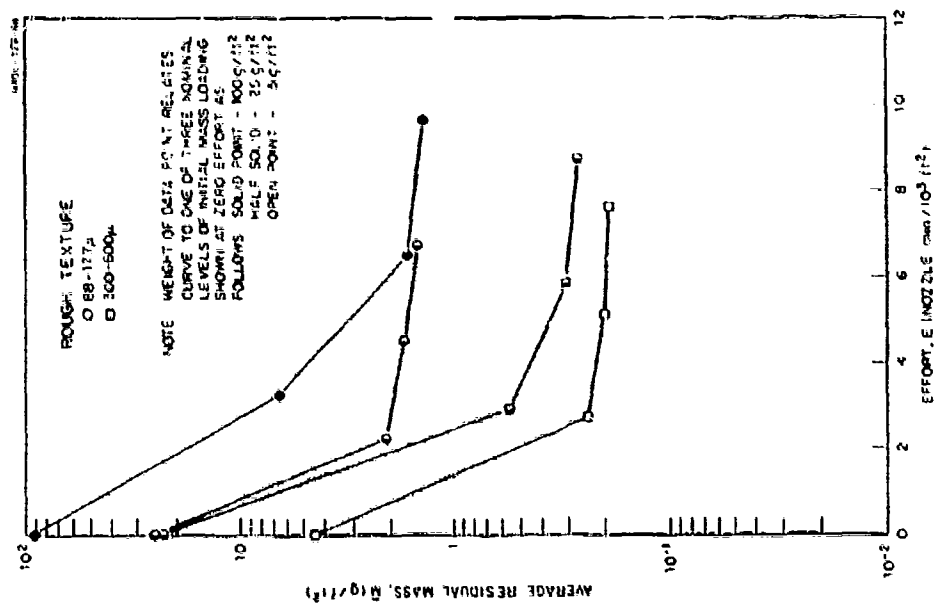


Fig. 3.4

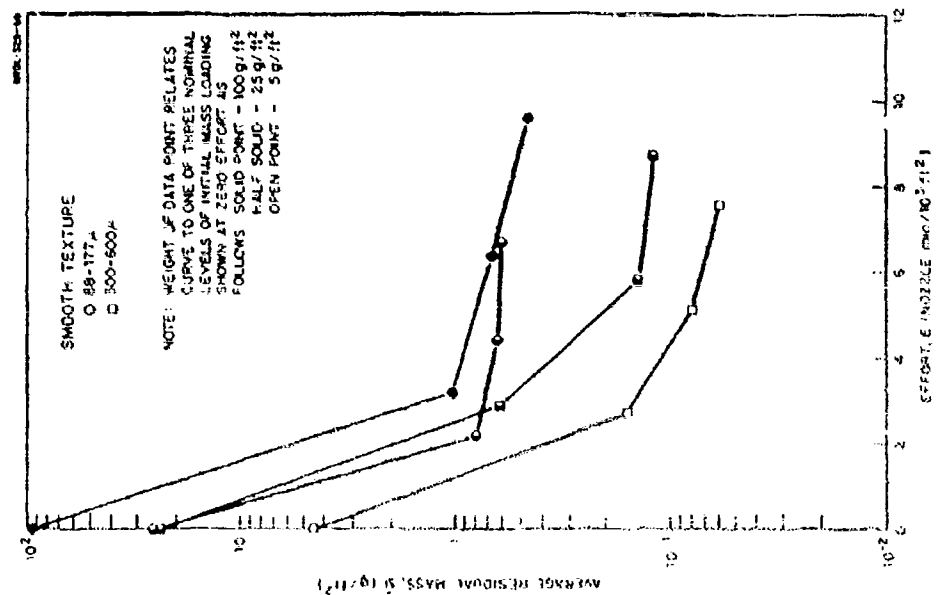


Fig. 3.3

Effects of Mass Loading and Particle Size Range on Full Scale Reclamation of an Asphalt Street for Two Surface Textures.

This is possible by noting the relative location of the fire nozzle curves in Figs. 3.1, 3.2 and 3.4. Such a comparison shows that, in general, the reclamation effectiveness at an engineering scale is an order of magnitude better than that achieved at full scale. In other words, the introduction of more realistic conditions involving increased equipment and operators prevents the effectiveness of full-scale tests from equalling that of smaller engineering-scale tests - no matter how much effort is invested. This points up the need for either extending reclamation studies to include full-scale tests of a number of methods and equipment not yet tested beyond the engineering scale or estimating the decreased effectiveness expected of full-scale reclamation.

### 3.2.2 Recovery Exposure

The planning of recovery operations requires estimating the exposure which recovery crews are expected to receive. These full-scale tests afforded an opportunity to estimate the exposure to firehosing teams and derive exposure reduction factors.

Exposure Reduction Factor,  $RN_2$ . A suitable formula for calculating recovery crew exposure has been available for some time.\* It is given in the simple form

$$D_2' = RN_2 D_2 \quad (1)$$

where  $D_2'$  is the actual recovery crew exposure.

$D_2$  is the potential exposure during the reclamation period, if the original field were unaffected by the reclamation effort.  
 $RN_2$  is the exposure reduction factor.

By rearranging terms, a convenient working equation can be written which shows how  $RN_2$  values are estimated from experimental results.

$$RN_2 = \frac{D_2'}{D_2} = \frac{\sum (I_j \Delta t_j)}{I_0 t} \quad (2)$$

the product  $I_j \Delta t_j$  represents the area of an incremental strip under an operator exposure-rate history curve (refer to Fig. 3.5).  $I_0$  is the average initial exposure rate in the contaminated area, and  $t$  is the total time of the recovery operation. Experimental values of  $I_0$  are

\*The derivation is given in Ref. 9. Experimental applications are shown in Refs. 6 and 7.

obtained from survey readings taken along the path a given operator is expected to take through the contaminated area. When this path cannot be reasonably predicted,  $I_0$  is calculated from a grid survey of the complete area. In the case of firehosing isolated areas (as in these full scale tests), team members will never be subjected to  $I_0$ . The bulk of the fallout simulant continuously recedes along a front located 20 to 30 ft away from the nozzle operator. Therefore, the firehosing team is never exposed to a radiation dose rate equal to  $I_0$ . In a real fallout situation, however, the contributions from contaminated surroundings could offset any gains resulting from the reduction of an  $I_0$  in an isolated area due to firehosing (or any other method). Refs. 4, 6 and 9 treat these more complex radiological situations in considerable detail.

Exposure Rate History. In order to obtain values for the numerator of Eq. 2, exposure rate histories were taken of all four fullscale firehosing tests. Frequent measurements were made of the changing gamma exposure rate with 27-F radiacs close to each nozzleman and the tow truck operator during the 10-to-14 min time interval. These exposure rate history plots are presented in Figs. 3.5 through 3.8, and the results are summarized in Table 3.1.

Table 3.1 is a solution to Eq. 2 in terms of  $RN_2$  values for the various starting conditions and tasks. Comparing the results associated with the nozzle men, the  $RN_2$  values identified with the rough and smooth surfaces differ by an amount ranging from 9 to 23 %. However, there are no apparent trends in the  $RN_2$  value attributable to surface texture. Furthermore, neither particle size range nor mass loading has any marked effect upon the magnitude of the exposure reduction factor for either the nozzle man or the tow truck operator.

Each set of exposure rate history curves in Fig. 3.5, 3.6 and 3.7 exhibit the same characteristic shapes and relative orientation among the curves. Fig. 3.8 shows a severe departure from this pattern as evidenced in the sharp peaks in all three history curves. These increases in exposure rate are due to the heavy accumulation of simulant deposited midway through the test as explained in Section 2.5.2b. Thus, heavy mass loadings (such as the 100 g/ft<sup>2</sup> concentration) can be expected to cause peaks in exposure rate histories.

This does not necessarily imply that resultant  $RN_2$  factors will increase. For the test in question  $RN_2$  factors for the nozzle men are near the average values shown at the bottom of Table 3.1. On the other hand the  $RN_2$  value for the tow truck operator is the largest among the four tests (30% greater than the average). Due to vehicular shielding,  $RN_2$  values for tow truck operators are 1/4 to 1/2 that of the nozzle men.

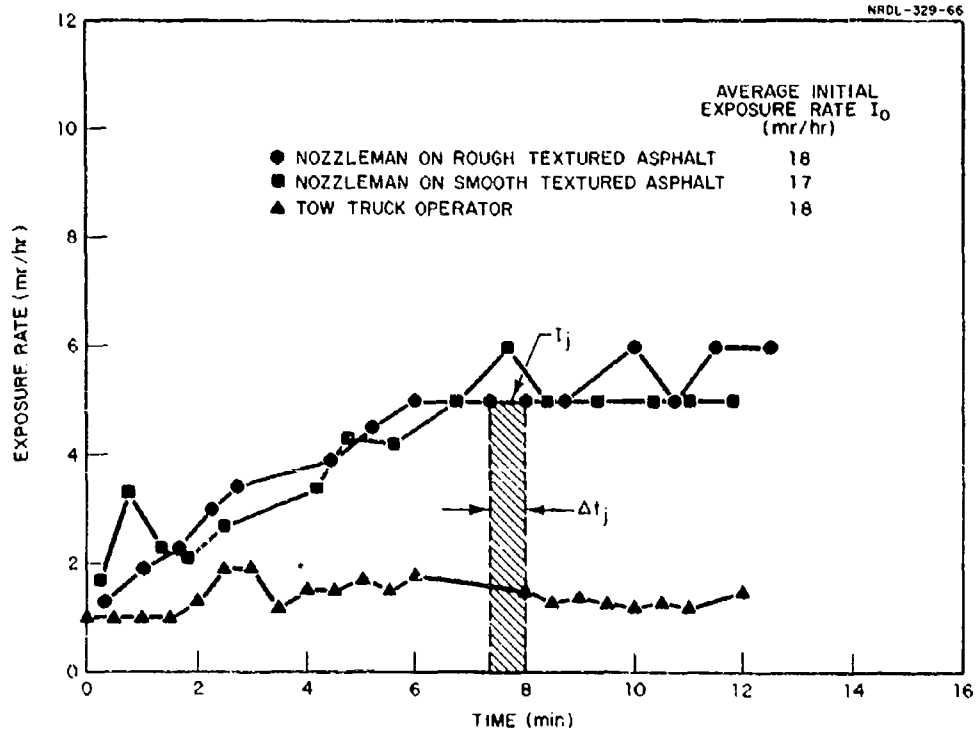


Fig. 3.5 Exposure Rate History for Recovery of Asphalt Pavement by Firehosing; Full Scale Test, 300-600 $\mu$ , 4.4 g/ft<sup>2</sup>.

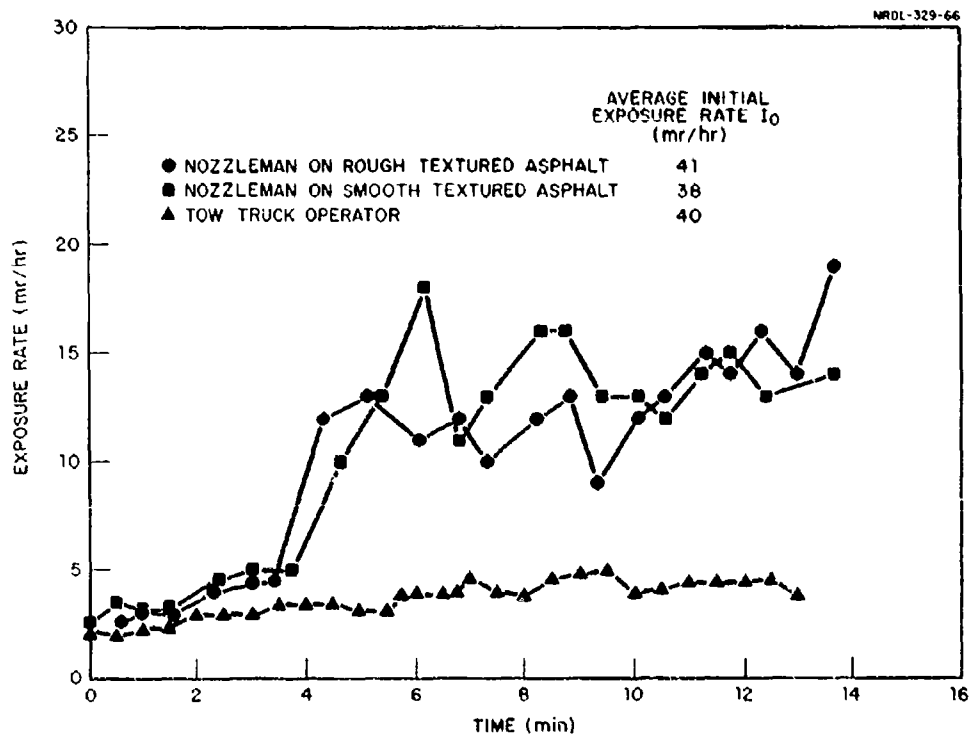


Fig. 3.6 Exposure Rate History for Recovery of Asphalt Pavement by Firehosing; Full Scale Test, 300-600 $\mu$ , 24.24 g/ft<sup>2</sup>.

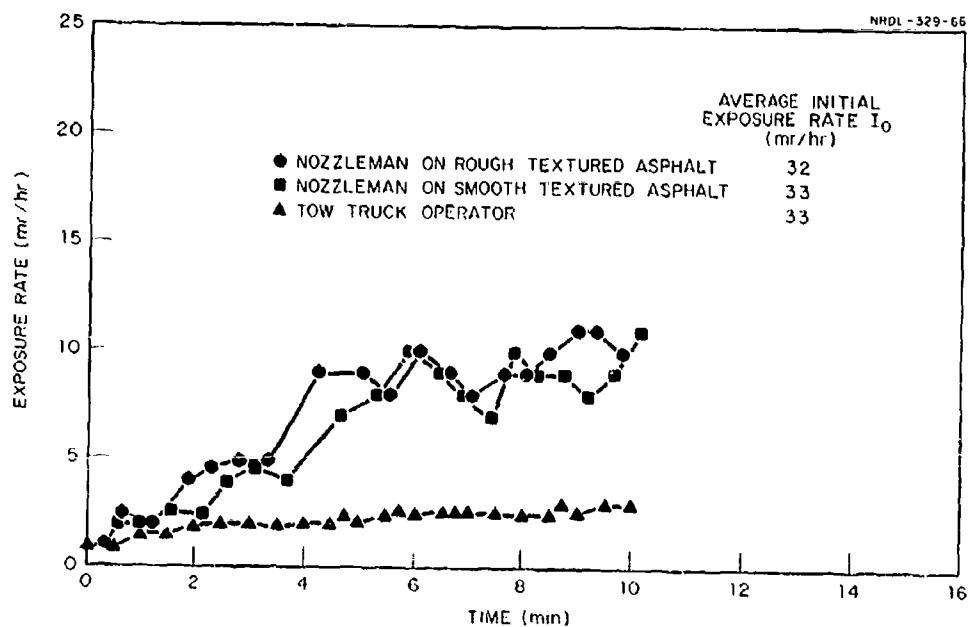


Fig. 3.7 Exposure Rate History for Recovery of Asphalt Pavement by Firehosing; Full Scale Test, 88-177u, 25.02 g/ft<sup>2</sup>.

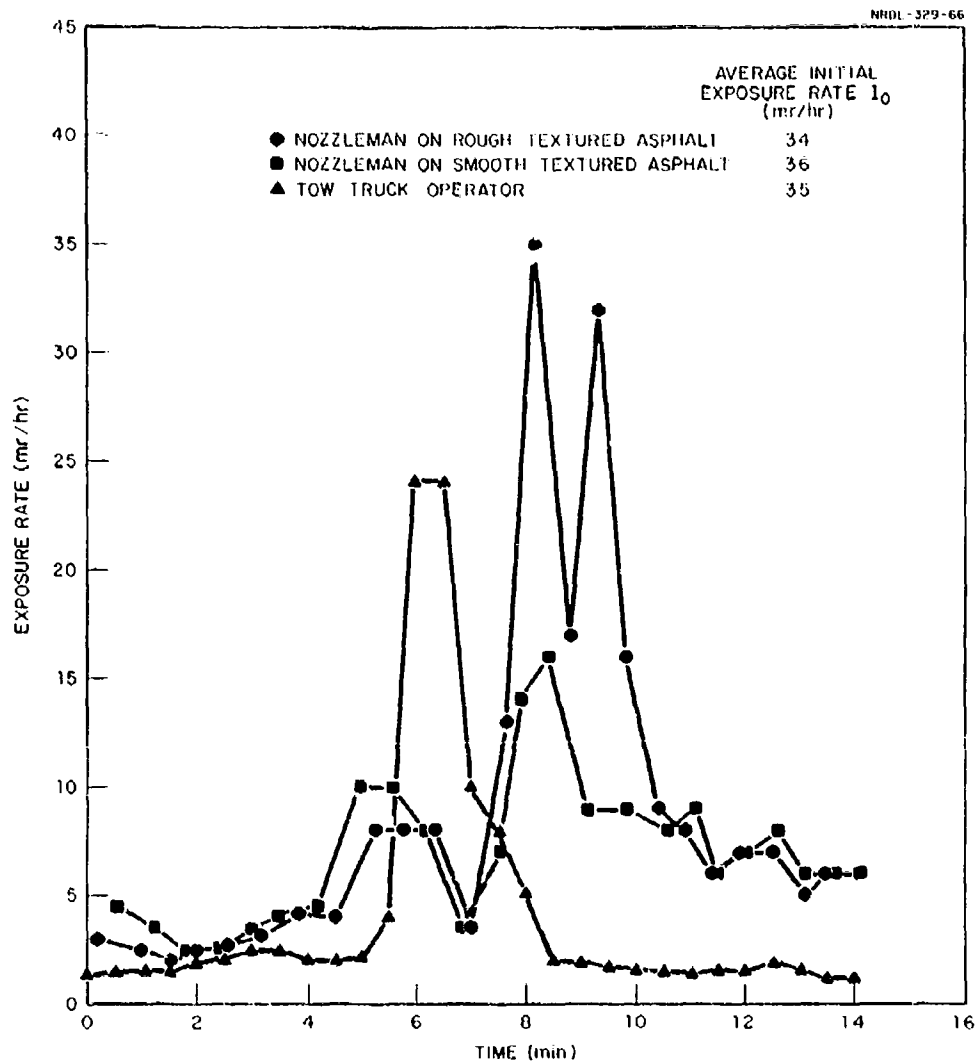


Fig. 3.8 Exposure Rate History for Recovery of Asphalt Pavement by Firehosing; Full Scale Test, 88-177 $\mu$ , 92.4 g/ft<sup>2</sup>.

TABLE 3.1

Recovery Exposure-Reduction Factor,  $RN_2$ , for Firehosing Crews - Full Scale Tests, Asphalt Pavement Test Area: 8,960 ft<sup>2</sup> (32 X 280 ft)

Recovery Task	Surface Texture	Initial Mass Loading, $M_0$ (g/ft <sup>2</sup> )	Recovery Interval (hr)	Initial Exposure Rate $I_0$ (mr/hr)	Potential Exposure $D_2$ (mr)	Actual Exposure $D_2$ (mr)	Exposure Reduction Factor, $RN_2$
<u>Particle Size Range 88-177 <math>\mu</math></u>							
Nozzleman	Rough	25.02	0.16	32.	5.1	1.1	0.22
Nozzleman	Smooth	25.02	0.16	33.	5.3	1.3	0.24
Tow Operator		25.02	0.17	33.	5.6	0.36	0.064
Nozzleman	Rough	92.40	0.225	34.	7.7	2.1	0.27
Nozzleman	Smooth	92.40	0.225	36.	8.1	1.8	0.22
Tow Operator		92.40	0.23	35.	8.0	0.94	0.12
<u>Particle Size Range 300-600 <math>\mu</math></u>							
Nozzleman	Rough	4.43	0.20	18.	3.6	0.76	0.21
Nozzleman	Smooth	4.43	0.20	17.	3.4	0.82	0.24
Tow Operator		4.43	0.20	18.	3.8	0.28	0.074
Nozzleman	Rough	24.24	0.23	41.	9.4	2.3	0.24
Nozzleman	Smooth	24.24	0.23	38.	8.7	2.5	0.29
Tow Operator		24.24	0.22	40.	8.8	0.85	0.097
<u><math>RN_2</math> Average for Test Series</u>							
Nozzleman	Rough						0.24
Nozzleman	Smooth						0.25
Tow Operator							0.089



one being reclaimed would continue to contribute to the crew exposure until the entire recovery operation was completed.

### 3.3 FIREHOSING OF ROOFING MATERIALS

These tests compare the reclamation effectiveness of the fire and flare nozzles on the following roofing materials: composition shingle, corrugated metal, fiberglass, and asphaltum. The reduced data are compiled in Tables A.5-A.16 and are plotted as performance curves in Figs. 3.9-3.26, showing residual mass as a function of effort.

#### 3.3.1 Effects of Nozzle Design and Roofing Material

The effects of nozzle design and roofing material on reclamation by firehosing are shown in Figs. 3.9-3.16 for particle size range 88-177  $\mu$ . Figures 3.17-3.20 show these same effects for particle size range 300-600  $\mu$ . Generally, the curves were consistently paired according to nozzle design with the flare nozzle being more effective than the fire nozzle. Two exceptions occur in Figs. 3.16 and 3.20 for corrugated metal where the difference in performance due to nozzle design is not significant.

From the consistent spacing between the appropriate curves from each pair of figures it is obvious that removal effectiveness is a direct function of surface roughness. Therefore the roofing materials may be ranked in order of decreasing effectiveness according to their increasing surface roughness: (1) fiberglass, (2) asphaltum, (3) corrugated metal, and (4) composition shingle. An exception to this ranking is depicted in Fig. 3.10 when fiberglass appeared to be no better than composition shingle. However, it was discovered that the panel used in this test was not completely cured. As a result some simulant became permanently imbedded in the epoxy layer softened by the heat of the sun. This would not have happened if the epoxy had been mixed in the correct proportions.

The adhesion of the asphaltum to the smooth plywood surface was so poor that the force of the fire nozzle stream eventually ruined the panels. This resulted in a loss of some data points - in particular see odd-numbered Figs. 3.11 through 3.17 inclusive. If this material would adhere tightly to an unfinished surface it would be almost as easy to clean as fiberglass and much easier and more economical to apply.

It will be noted in Fig. 3.10, 3.11, 3.13, 3.17 and 3.18 that there are five curves exhibiting a positive slope after the first pass. This reversal in slope occurs only for those combinations of nozzle design and roofing material that result in maximum removal effectiveness. For this reason none of these curves involve the fire nozzle or composition shingles.

Because each of the curves in question changes slope at very low values of residual mass ( $0.15 \text{ g/ft}^2$  or less) and, hence, at proportionately low counting rates, it is suspected that the shielded detector was operating in a region approaching its lower limit of counting reliability. The fact that at least four other curves (see Fig. 3.9, 3.12, 3.19 and 3.20), based on data obtained in comparably low counting regions, exhibit negative slopes in no wise weakens such a conclusion. This is precisely the random results to be expected when counting reliability becomes marginal.

Because the slope reversal of the curves might also be caused by the statistical uncertainty in the data points, the standard deviations of the residual masses were estimated for all the curves cited. In five cases the deviations were large enough to permit a change in slope. That is: the three curves in Figs. 3.10, 3.11 and 3.17 could have been negative, and the two in Figs. 3.19 and 3.20 positive. However, this does not apply to the remaining four curves. The positive slopes of the two curves in Fig. 3.13 and 3.18, therefore, must be blamed on low counting reliability.

### 3.3.2 Mass Loading and Particle Size Effects

The effects of mass loading and particle size on nozzle performance are illustrated by the performance curves in Figs. 3.21-3.26. These figures are arranged by surface material and paired to show differences due to nozzle design.

A cursory examination of these curves reveals two consistent trends that are generally true for the three roofing materials represented. First, the flare nozzle is more effective than the fire nozzle, especially when encountering the smaller particle size range ( $88\text{-}177 \mu$ ) at mass loadings less than  $100 \text{ g/ft}^2$ . Second, performance curves for the  $88\text{-}177 \mu$  size range tend to reach what appears to be a minimum residual level after three passes. In most of these cases, the additional effort required is not justified by the small decrease in residual mass achieved by the third pass.

No general statements can be made concerning the influence of particle size upon hosing effectiveness, since only one mass loading ( $25 \text{ g/ft}^2$ ) was tested for both size ranges. However, for this one value, all the performance curves from Fig. 3.21 to 3.26 show that the larger  $300\text{-}600 \mu$  particles were more effectively removed by either nozzle. This is consistent with the findings from the tests on asphalt streets.

The effects of mass loading on the firehosing performance varied according to surface roughness, particle size and nozzle design. For the larger 300-600  $\mu$  size range, mass loading showed little influence on hosing performance, except in two cases. These are evident in Figs. 3.24 and 3.25 involving the flare nozzle on corrugated metal and the fire nozzle on composition shingles. The generous separation between paired curves shows that the 5 g/ft<sup>2</sup> mass loading was consistently cleaned more effectively than the 25 g/ft<sup>2</sup> mass loading at all hosing passes.

The varied effects of mass loading on the small 88-177  $\mu$  size range are evident for two of the three roof materials:

Fiberglass. In the case of fiberglass, Fig. 3.21 demonstrates clearly by the superposition of the fire nozzle curves that mass loading has no effect on residual mass. The lack of data points in Fig. 3.22 does not allow for any related conclusions on the part of flare nozzle performance.

Corrugated Metal. Figures 3.23 and 3.24 indicate a definite correlation between initial and residual mass at the 88-177  $\mu$  size range. The fire nozzle curves (Fig. 3.23) pair up so that small mass loadings of 25 g/ft<sup>2</sup> and less always exhibit lower residual mass values than do mass loadings of 50 g/ft<sup>2</sup> and greater. An even stronger relationship between initial and residual mass is shown in Fig. 3.24 for the flare nozzle by the sequential spacing of the performance curves.

Composition Shingles. The fire nozzle performance curves are shown in Fig. 3.25. For particle size range 88-177  $\mu$ , the performance curves do not seem to fall in a consistent relation to each other that can be explained by the initial mass loading. The mixed relationship of the curves may be due to deposition of some simulant under the shingle tabs. This is known to happen but only in a non-uniform and highly unpredictable manner. The flare nozzle curves in Fig. 3.26 are arranged in such a way that no mass loading effects are evident over the range of initial values from 12 to 50 g/ft<sup>2</sup>. From the relation of the three superimposed curves to the one uppermost in Fig. 3.26, it is apparent that residual values associated with mass loadings of 100 g/ft<sup>2</sup> are consistently greater than for those attributed to smaller mass loadings.

It should be pointed out that, with few exceptions, all the remarks concerning removal effectiveness have been mass-oriented. That is, comparisons have been made with respect to residual mass. The latter is a measure of absolute effectiveness and was best suited to the purposes of this report. For operating manuals, however, the residual fraction (F) is preferred. F is the ratio of the residual mass to the initial mass and, therefore, is a measure of relative effectiveness. This quantity has been reported (along with residual mass) in the tables of Appendix A.

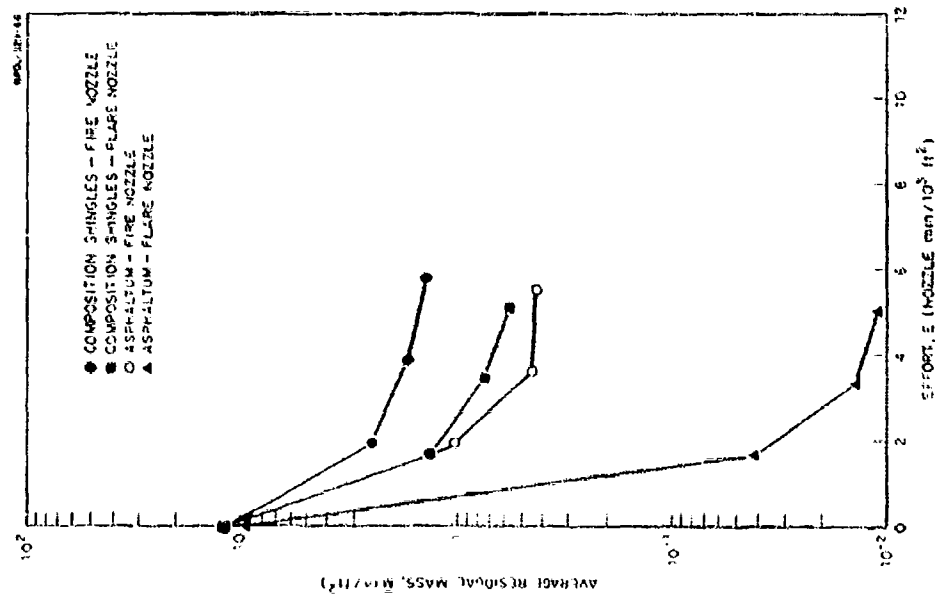


Fig. 3.9

Comparison of Nozzle Design and Roofing Material Effects for Particle Size Range 88-177 $\mu$  at a Mass Loading of 12.0 g/ft<sup>2</sup>.

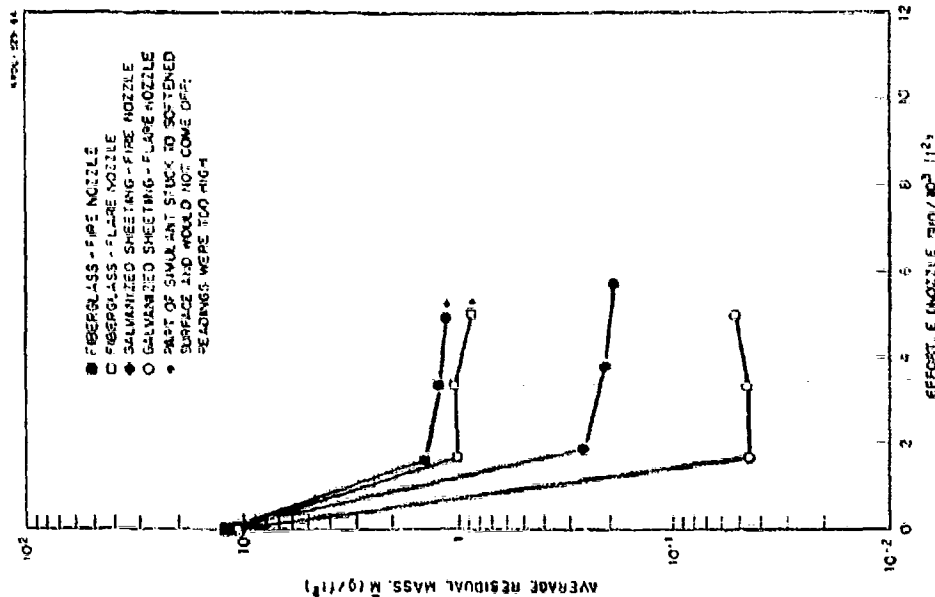


Fig. 3.10

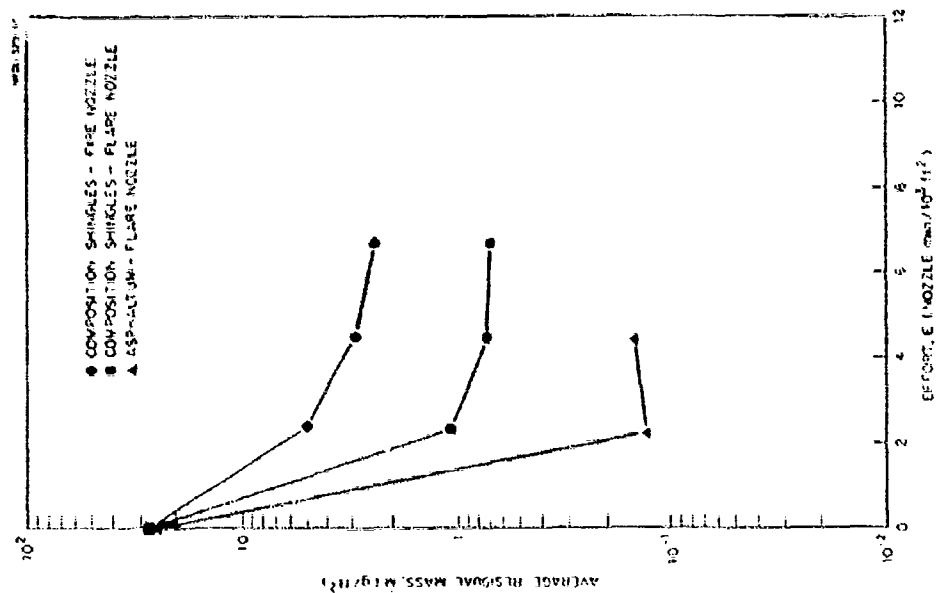


Fig. 3.11

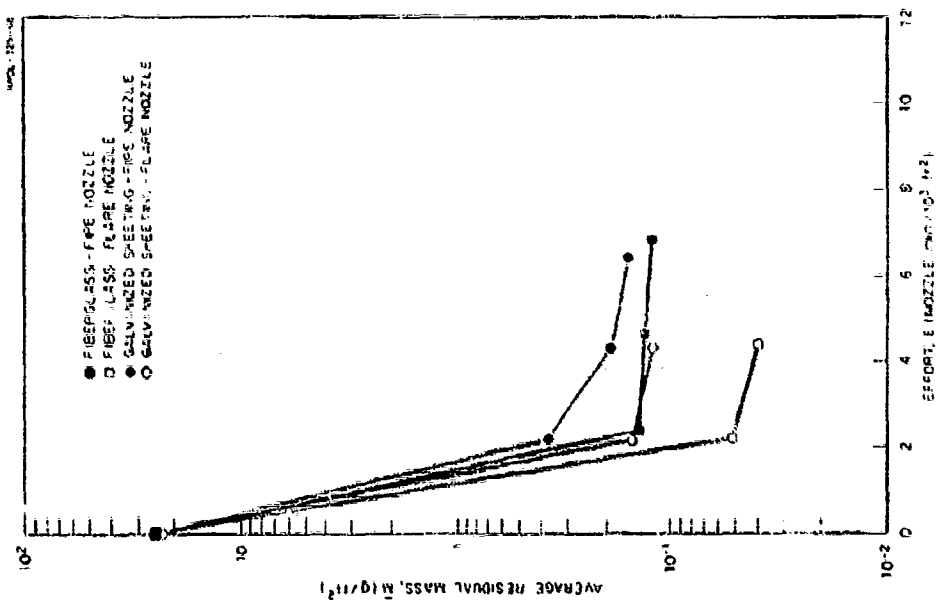


Fig. 3.12

Comparison of Nozzle Design and Roofing Material Effects for Particle Size Range 88-177 $\mu$  at a Mass Loading of 25.0 g/ft<sup>2</sup>.

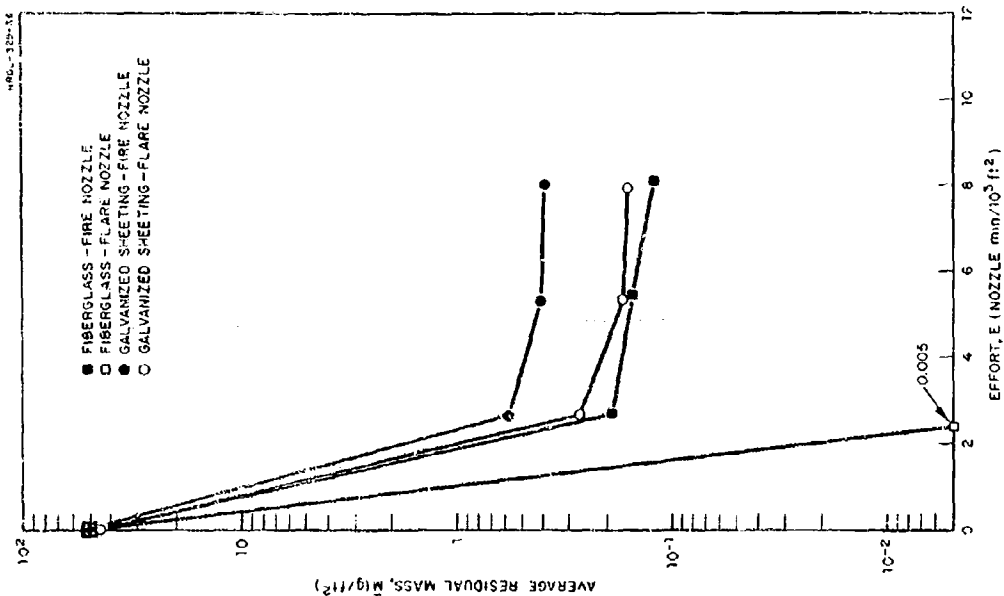


Fig. 3.13

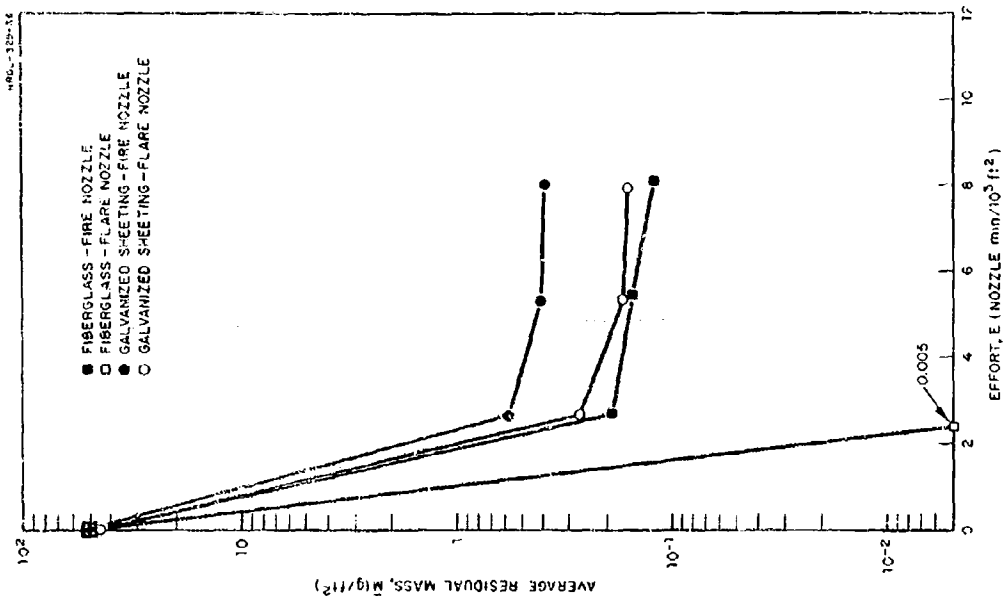


Fig. 3.14

Comparison of Nozzle Design and Roofing Material Effects for Particle Size Range 68-177 $\mu$  at a Mass Loading of 50.0 g/ft<sup>2</sup>.

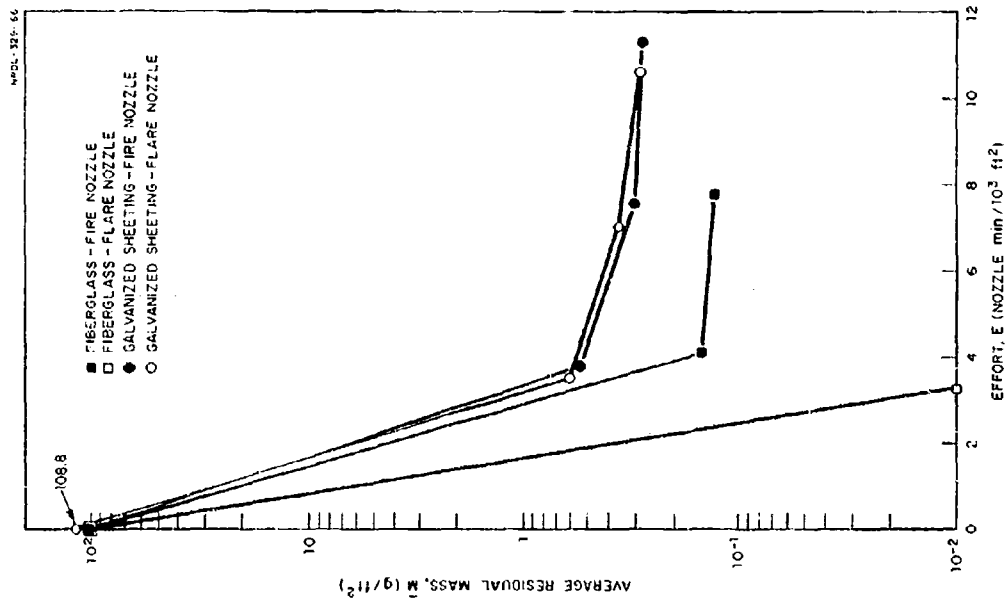


Fig. 3.15  
Comparison of Nozzle Design and Roofing Material Effects for Particle Size Range 88-177 $\mu$  at a Mass Loading of 100.0 g/ft<sup>2</sup>.

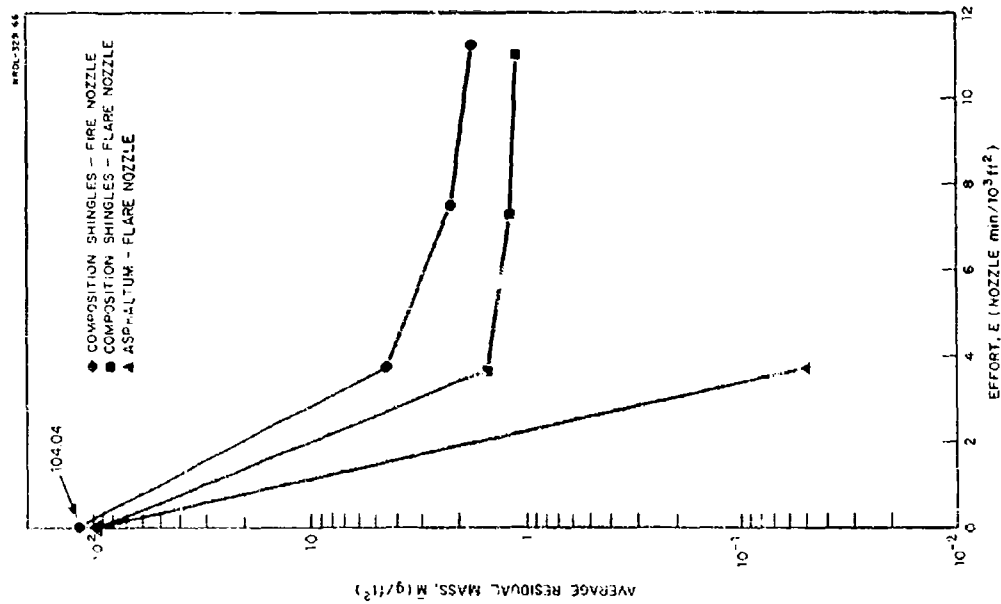


Fig. 3.16

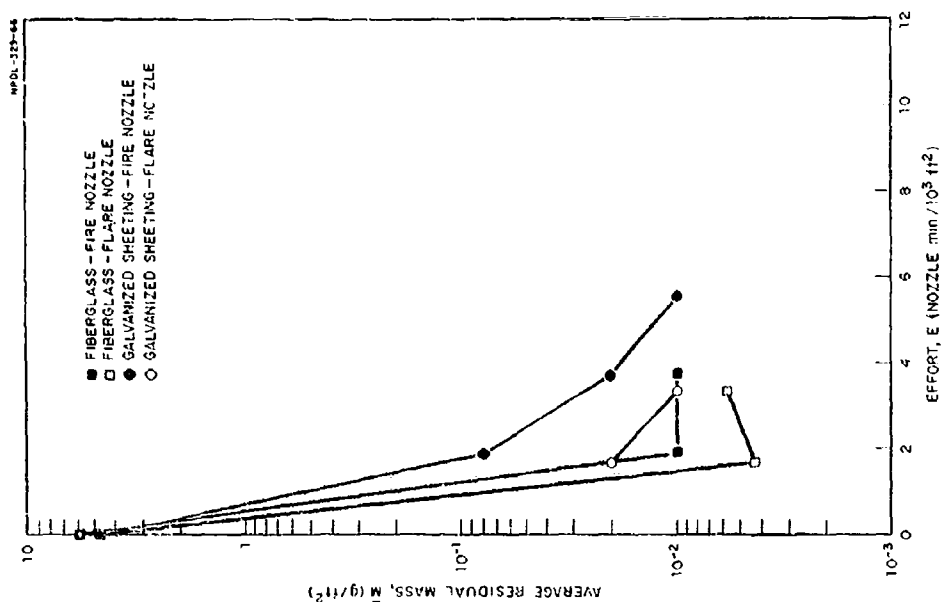


Fig. 3.18

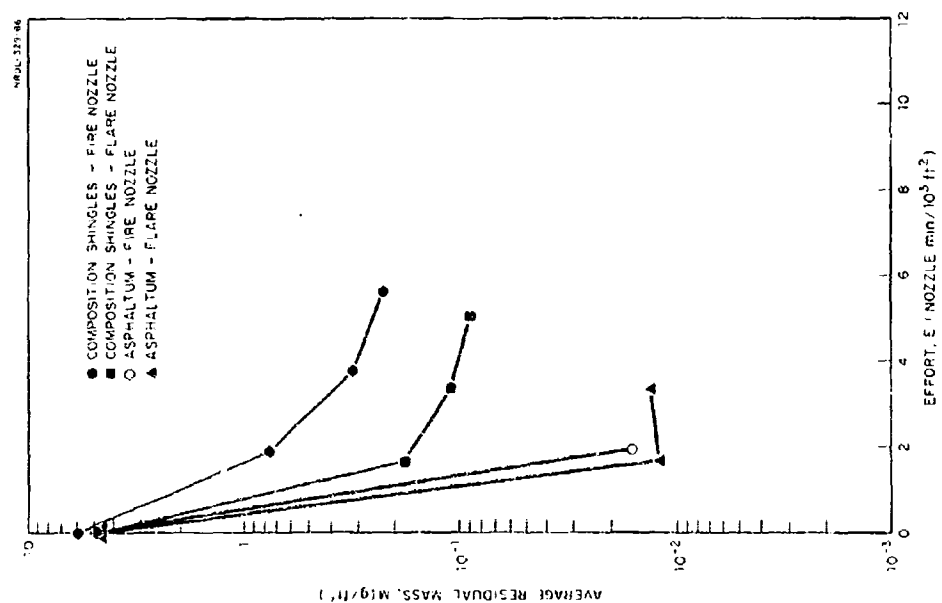


Fig. 3.17

Comparison of Nozzle Design and Roofing Material Effects for Particle Size Range 300-600 $\mu$  at a Mass Loading of 5.0 g/ft<sup>2</sup>.



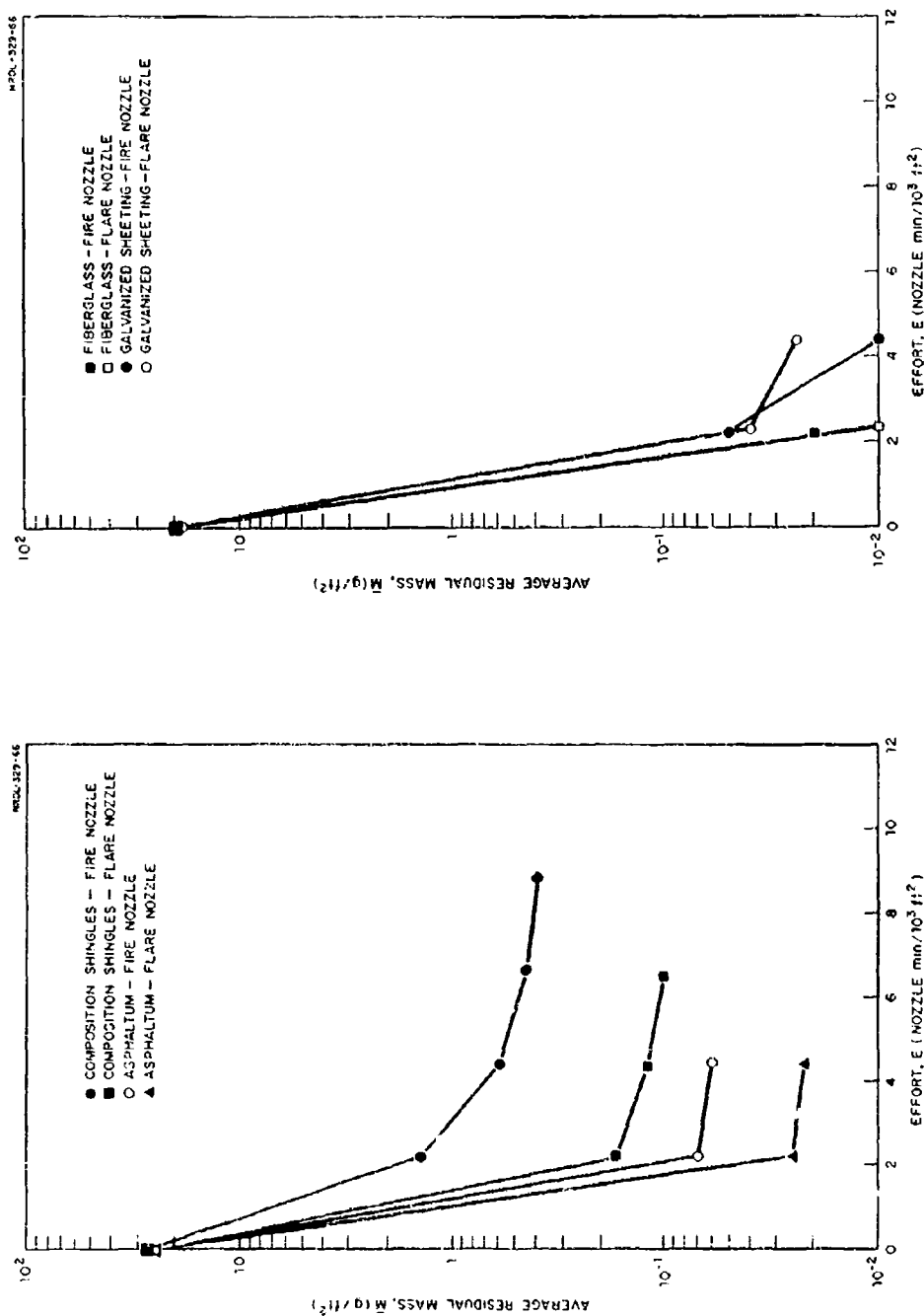


Fig. 3.19 Comparison of Nozzle Design and Roofing Material Effects for Particle Size Range 300-600 $\mu$  at a Mass Loading of 25.0 g/ft<sup>2</sup>.

Fig. 3.20

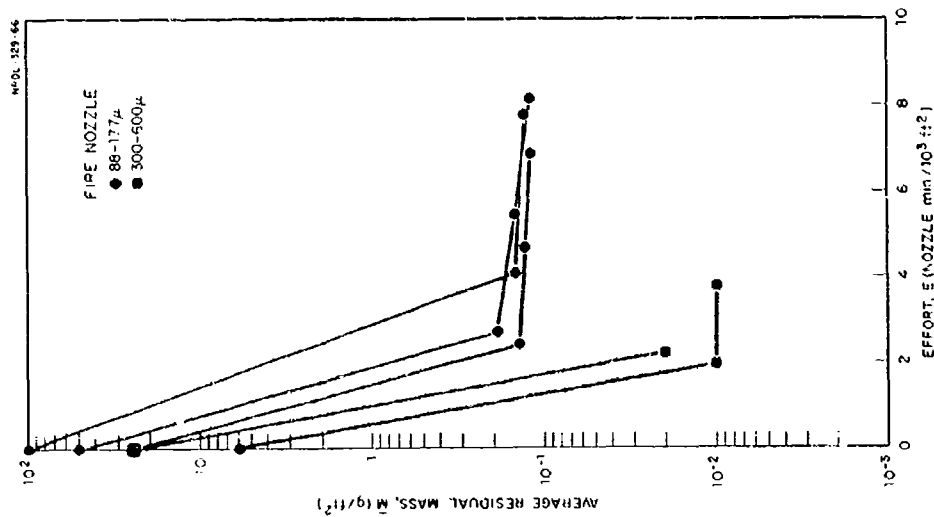
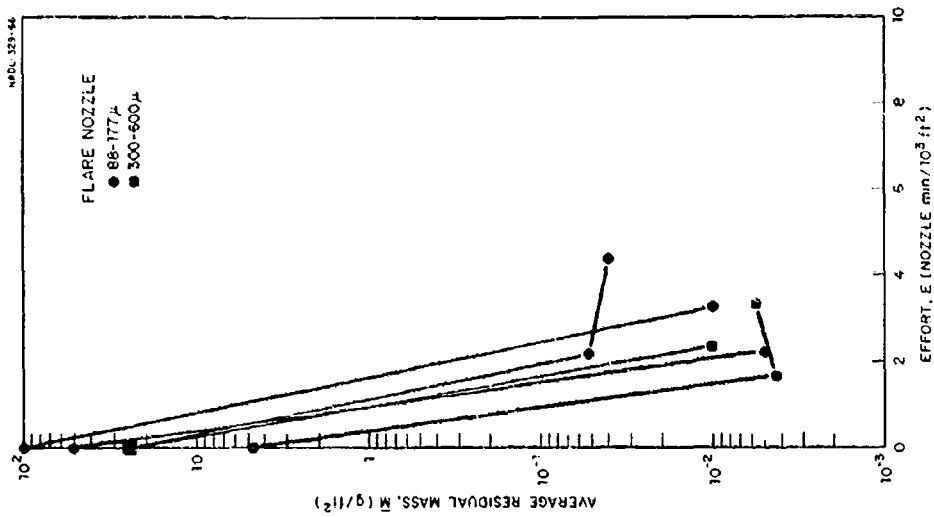


Fig. 3.21  
Comparison of the Effects of Mass Loading and Particle Size Range on Hosing Performance for Two Nozzle Designs on Fiberglass Roofing Material.

Fig. 3.22

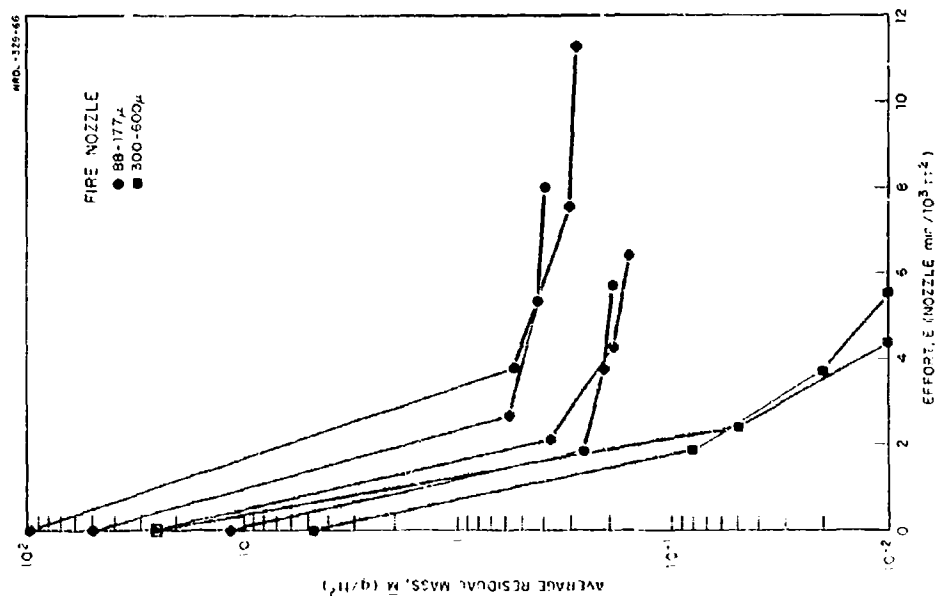


Fig. 3.23

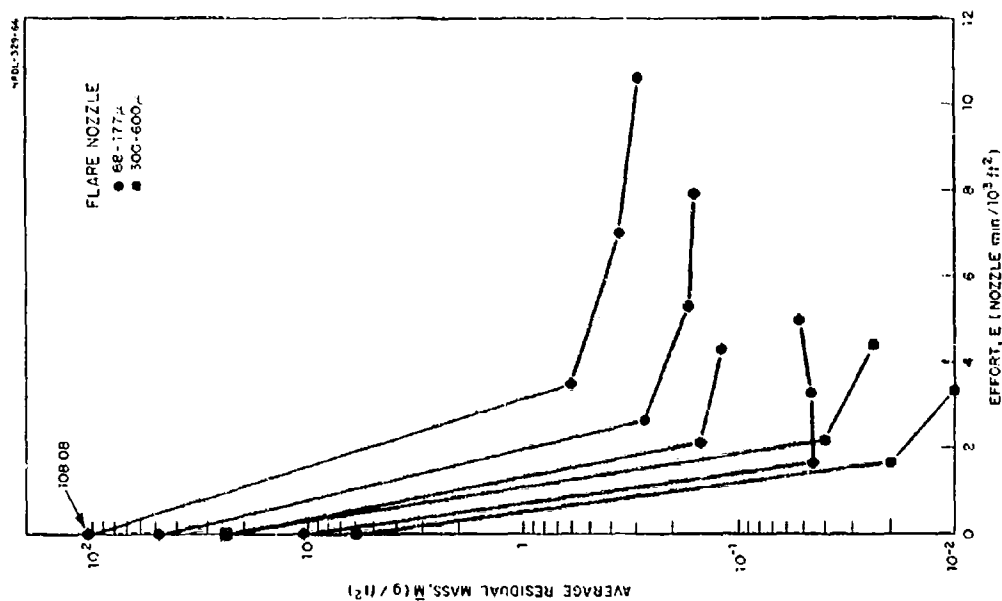


Fig. 3.24

The Effects of Mass Loading and Particle Size Range on Hosing Performance of the Fire Nozzle on Corrugated Metal Roofing Material.

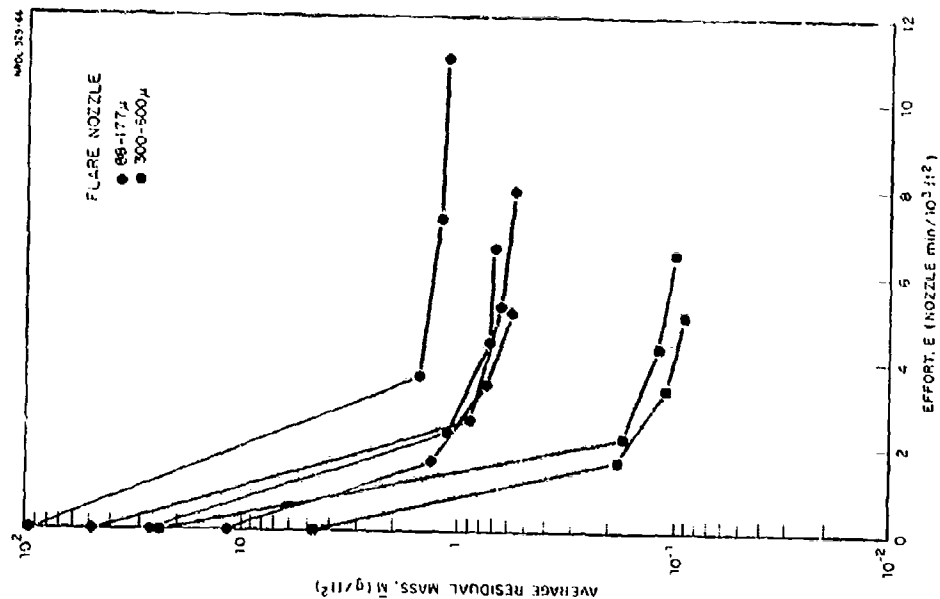


Fig. 3.26

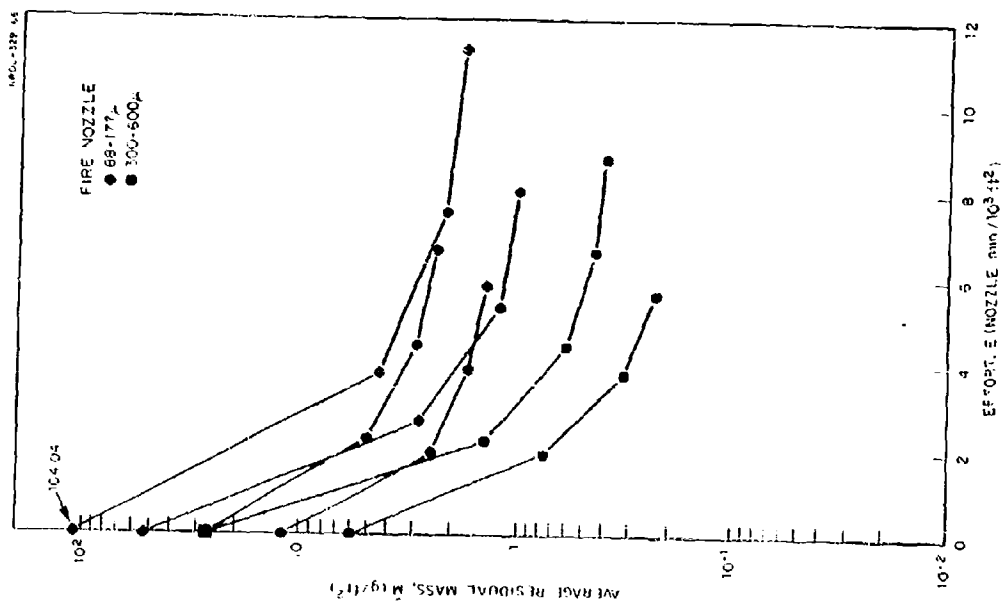


Fig. 3.25

Comparison of the Effects of Mass Loading and Particle Size Range on Hosing Performance of Two Nozzle Designs on Composition Shingle Roofing Material.

## SECTION IV

### CONCLUSIONS

In general, it may be concluded for both asphalt pavements and roofing materials that:

1. Effectiveness of reclamation by firehosing improves as surface roughness decreases.

2. Larger (300-600  $\mu$ ) particle sizes are more easily removed than the smaller (88-177  $\mu$ ) particle sizes.

3. Removal effectiveness improves with effort, but the residual mass is not significantly reduced after the second pass.

4. The effect of mass loading upon firehosing effectiveness is not predictable because it varies with surface roughness, particle size and nozzle design.

During the engineering-scale tests on asphalt, the flare nozzle failed to exhibit a reclamation performance that was consistently superior to the standard fire nozzle for a significant number of the combinations of mass loading and particle size tested.

The full-scale tests on asphalt showed that operational factors prevent the reclamation effectiveness from ever equaling that achieved at an engineering scale - no matter how much effort is expended. From the exposure rate histories it was found that the exposure reduction factor ( $RN_2$ ) for either the nozzle man or the vehicle operator is not significantly influenced by pavement surface roughness, fallout particle size or mass loading.

The roof firehosing tests demonstrated the superiority of the flare nozzle as a reclamation tool. Fiberglass showed great potential as a durable, easy-to-clean roofing material.

## SECTION V

### RECOMMENDATIONS

From the results and conclusions obtained in the series of fire-hosing tests, the following recommendations are made.

1. Investigate feasibility of manufacture and distribution of NRDL flare nozzles to recoverable communities and facilities located in potential fallout areas.

2. If (1) is feasible, employ the NRDL flare nozzle on roofs and in confined paved areas where it is not possible to take advantage of the long reach of the water stream characteristic of fire nozzles.

3. Consider the use of smoother surfaces, such as fiberglass-epoxy, for roofs on vital structures that are likely to require reclamation soon after being contaminated by fallout.

4. Conduct tests on roofing materials at a larger and more realistic scale, or find a suitable method for making operational adjustments to the limited-scale test results. Include the technique of lobbing nozzled water streams from ground level as part of these tests.

#### REFERENCES

1. F. S. Vine, et al, "Methods and Procedures for the Reclamation of Land Targets," U. S. Naval Radiological Defense Laboratory Report USNRDL-407, 5 March 1953.
2. J. D. Sartor, et al, "Cost and Effectiveness of Decontamination Procedures for Land Targets," U. S. Naval Radiological Defense Laboratory Report USNRDL-TR-196, 27 Dec. 1957.
3. W. L. Owen, J. D. Sartor, W. H. Van Horn, "Performance Characteristics of Wet Decontamination Procedures," U. S. Naval Radiological Defense Laboratory Technical Report, USNRDL-TR-335, 21 July 1960.
4. C. F. Miller, "Fallout and Radiological Countermeasures", Vol. I, Stanford Research Institute, SRI Project No. IM-4021, Jan. 1963.
5. D. E. Clark Jr. and W. C. Cobbin, "Some Relationships Among Particle Size, Mass Level and Radiation Intensity of Fallout From a Land Surface Nuclear Detonation," U. S. Naval Radiological Defense Laboratory, USNRDL-TR-639, 21 March 1963.
6. W. L. Owen and J. D. Sartor, "Radiological Recovery of Land Target Components, Complex III," U. S. Naval Radiological Defense Laboratory, USNRDL-TR-700, 20 Nov. 1963.
7. W. C. Cobbin, W. L. Owen, "Development and Test of a Sod Removal Procedure for Moist Lawns Contaminated by Simulated Fallout," U. S. Naval Radiological Defense Laboratory, USNRDL-TR-965, 10 April 1965.
8. D. E. Clark and W. C. Cobbin, "Removal of Simulated Fallout From Pavements by Conventional Street Flushers," U. S. Naval Radiological Defense Laboratory Technical Report, USNRDL-TR-797, 18 June 1964.
9. H. Lee, "Estimating Cost and Effectiveness of Decontaminating Land Targets," U. S. Naval Radiological Defense Laboratory, USNRDL-TR-435, 6 June 1960.

## APPENDIX A

### REDUCED TEST DATA

All the foregoing firehosing performance curves were plotted from the data contained in Tables A.1 through A.16. The average initial mass loadings shown in these tables were calculated from the actual weight of material dispersed. Initial radiation and residual radiation values represent the averages of all survey stations for a given test area. The number of stations for each of the three experiments performed were: engineering scale - 18, full scale - 34, and roof panels - 2. Average counts were normalized to a  $Ce^{60}$  standard, decayed to an arbitrary zero time, and corrected for background. From these corrected counts and the known mass loading it was possible to derive the average residual mass and average residual fraction. For detailed explanation see Ref. 7, App. D.

It should be noted that two one-minute counts were taken at each station to guard against the collection of erroneous readings. The rate and effort values in the last two columns of the tables were calculated from time and motion studies.

Standard deviations in the residual mass values ranged from  $\pm 1$  to  $\pm 36$  percent. An approximate value of  $\pm 15\%$  may be taken as estimated average deviation.



TABLE A.1  
Engineering-Scale Performance Test Results for Flare Nozzle on Rough Asphalt Pavement

Nominal Mass Loading (g/ft <sup>2</sup> )	Average Initial Mass $\bar{M}_0$ (g/ft <sup>2</sup> )	Average Initial Radiation $\bar{I}_0$ (cpm)	Pass No.	Average Residual Radiation $\bar{I}$ (cpm)	Average Residual Mass $\bar{M}$ (g/ft <sup>2</sup> )	Average Residual Fraction $\bar{F}$	Time per Pass t (min)	Rate of Removal R (ft <sup>2</sup> /min)	Cumulative Effort E ( $\frac{\text{Noz Min}}{103 \text{ ft}^2}$ )
Particle Size Range, 88-177 $\mu$									
5.0	5.04	25,593	1	928	0.18	0.0362	2.10	600	1.67
			2	512	0.10	0.0200	2.05	615	3.29
			3	348	0.07	0.0136	2.00	630	4.88
25.0	26.12	156,824	1	1,247	0.21	0.0080	2.37	532	1.88
			2	556	0.09	0.0035	2.03	621	3.49
100.0	95.77	523,866	1	2,560	0.47	0.0049	3.68	285	3.50
			2	1,260	0.23	0.0024	3.50	300	6.84
			3	1,017	0.18	0.0019	3.52	298	10.14
Particle Size Range, 300-600 $\mu$									
5.0	5.22	41,585	1	1,191	0.15	0.0286	2.30	548	1.82
			2	389	0.05	0.0093	2.30	548	3.65
			3	306	0.04	0.0074	2.30	548	5.48
25.0	24.86	199,446	1	1,380	0.17	0.0069	3.35	376	2.66
			2	604	0.07	0.0030	3.35	376	5.32
			3	389	0.05	0.0019	3.35	376	7.98

TABLE A.2

Engineering-Scale Performance Test Results for Fire Nozzle on Rough Asphalt Pavement (Extracted from 1963 firehosing test results)

Average Initial Mass $\bar{M}_0$ (g/ft <sup>2</sup> )	Pass No.	Average Residual Mass $\bar{M}$ (g/ft <sup>2</sup> )	Average Residual Fraction $\bar{F}$	Rate of Removal $R$ (ft <sup>2</sup> /min)	Cumulative Effort $E$ $\left( \frac{\text{Noz Min}}{103 \text{ ft}^2} \right)$
<u>Particle Size Range, 88-177 <math>\mu</math></u>					
3.76	1	0.63	0.169	484	2.07
	2	0.40	0.106	559	3.86
24.2	1	0.56	0.023	418	2.39
	2	0.34	0.014	496	4.41
102.5	1	0.71	0.007	346	2.89
	2	0.16	0.001	430	5.21
<u>Particle Size Range, 300-600 <math>\mu</math></u>					
4.09	1	0.04	0.009	462	2.16
	2	0.02	0.006	665	3.67
23.4	1	0.26	0.011	451	2.22
	2	0.08	0.003	596	3.89

TABLE A.3

Full Scale Performance Test Results for Standard Fire Nozzle on Smooth Asphalt Pavement

Nominal Mass Loading (g/ft <sup>2</sup> )	Average Initial Mass $\bar{M}_0$ (g/ft <sup>2</sup> )	Average Initial Radiation $\bar{I}_0$ (cpm)	Pass No.	Average Residual Radiation $\bar{I}$ (cpm)	Average Residual Mass $\bar{M}$ (g/ft <sup>2</sup> )	Average Residual Fraction $\bar{F}$	Time Per Pass $t$ (min)	Rate of Removal $R$ (ft <sup>2</sup> /min)	Cumulative Effort $E$ $\left(\frac{\text{Noz Min}}{103 \text{ ft}^2}\right)$
Particle Size Range, 88-177 $\mu$									
25.0	25.02	44,305	1	1,393	0.78	0.031	9.9	905	2.20
			2	1,092	0.62	0.025	10.0	896	4.44
			3	1,045	0.60	0.024	10.0	896	6.68
100.0	92.40	52,912	1	607	1.02	0.011	14.4	622	3.21
			2	388	0.65	0.007	14.5	618	6.45
			3	276	0.46	0.005	14.0	640	9.58
Particle Size Range, 300-600 $\mu$									
5.0	4.43	34,703	1	1,265	0.16	0.036	12.08	742	2.70
			2	664	0.08	0.019	10.75	833	5.10
			3	456	0.06	0.013	11.00	814	7.56
25.0	24.24	183,690	1	4,539	0.61	0.025	13.0	689	2.90
			2	1,150	0.14	0.006	13.0	689	5.80
			3	945	0.12	0.005	13.0	689	8.70

\*Rate is ft<sup>2</sup>/min for two teams using nozzle pressure of 75 psi.

TABIE A.4

Full Scale Performance Test Results for Standard Fire Nozzle on Rough Asphalt Pavement

Nominal Mass Loading (g/ft <sup>2</sup> )	Average Initial Mass $\bar{M}_0$ (g/ft <sup>2</sup> )	Average Initial Radiation $\bar{I}_0$ (cpm)	Pass No.	Average Residual Radiation $\bar{I}$ (cpm)	Average Residual Mass $\bar{M}$ (g/ft <sup>2</sup> )	Average Residual Fraction $\bar{F}$	Time per Pass $t$ (min)	Rate* of Removal $R$ (ft <sup>2</sup> /min)	Cumulative Effort $E$ $\left(\frac{\text{Noz Min}}{10^3 \text{ ft}^2}\right)$
Particle Size Range, 88-177 $\mu$									
25.0	25.02	47,394	1	3,978	2.10	0.084	9.9	905	2.20
			2	3,241	1.70	0.068	10.0	896	4.44
			3	2,819	1.48	0.059	10.0	896	6.68
100.0	92.40	45,430	1	3,165	6.47	0.070	14.4	622	3.21
			2	820	1.66	0.018	14.5	618	6.45
			3	689	1.39	0.015	14.0	640	9.58
Particle Size Range, 300-600 $\mu$									
5.0	4.43	46,481	1	2,528	0.24	0.054	12.08	742	2.70
			2	2,104	0.20	0.045	10.75	833	5.10
			3	2,060	0.19	0.044	11.00	814	7.56
25.0	24.4	204,479	1	4,672	0.56	0.023	13.0	689	2.90
			2	2,616	0.31	0.013	13.0	689	5.80
			3	2,165	0.27	0.011	13.0	689	8.70

\*Rate is ft<sup>2</sup>/min for two teams using nozzle pressure of 75 psi.

TABLE A.5

Limited Engineering Scale Performance Test Results for Fire Nozzle on Roofing Materials  
Particle Size Range 88-177  $\mu$ ; Nominal Mass Loading 12.0 g/ft<sup>2</sup>

Surface	Average Initial Mass $\bar{M}_0$ (g/ft <sup>2</sup> )	Average Initial Radiation $\bar{I}_0$ (cpm)	Pass No.	Average Residual Radiation $\bar{I}$ (cpm)	Average Residual Mass $\bar{M}$ (g/ft <sup>2</sup> )	Average Residual Fraction $\bar{F}$	Time per Pass $t$ (min)	Rate of Removal $R$ (ft <sup>2</sup> /min)	Cumulative Effort $E$ $\left(\frac{\text{Noz Min}}{103 \text{ ft}^2}\right)$
Asphaltum	11.82	36,182	1	2,279	1.04	0.06	0.37	518	1.93
			2	1,365	0.45	0.04	0.32	600	3.60
			3	1,324	0.43	0.04	0.32	600	5.53
Composition Shingle	11.82	42,248	1	3,830	2.47	0.21	0.37	518	1.93
			2	6,000	1.68	0.14	0.37	518	3.86
			3	4,945	1.38	0.12	0.37	518	5.79
Fiberglass	11.82	22,684	1	2,945	1.43	0.13	0.31	619	1.61
			2	2,536	1.23	0.11	0.32	600	3.28
			3	2,366	1.15	0.10	0.31	619	4.89
Corrugated Metal	11.82	38,661	1	925	0.26	0.02	0.35	548	1.82
			2	752	0.21	0.02	0.37	518	3.75
			3	668	0.19	0.02	0.37	518	5.68

TABLE A.6

Limited Engineering Scale Performance Test Results for Fire Nozzle on Roofing Materials  
Particle Size Range 88-177  $\mu$ ; Nominal Mass Loading 25.0 g/ft<sup>2</sup>

Surface	Average Initial Mass $\bar{M}_0$ (g/ft <sup>2</sup> )	Average Initial Radiation $\bar{I}_0$ (cpm)	Pass No.	Average Residual Radiation $\bar{I}$ (cpm)	Average Residual Mass $\bar{M}$ (g/ft <sup>2</sup> )	Average Residual Fraction $\bar{F}$	Time per Pass $t$ (min)	Rate of Removal $R$ (ft <sup>2</sup> /min)	Cumulative Effort $\Sigma$ $\left(\frac{\text{Noz Min}}{10^3 \text{ ft}^2}\right)$
Asphaltum									
Composition Shingle	27.19	80,573	1	14,912	5.03	0.18	0.43	446	2.24
			2	8,608	2.90	0.11	0.41	468	4.43
			3	7,004	2.36	0.09	0.41	468	6.62
Fiber-glass	24.83	73,539	1	412	0.14	0.006	0.46	417	2.40
			2	377	0.13	0.005	0.43	446	4.84
			3	368	0.12	0.005	0.42	457	6.83
Corrugated Metal	24.83	80,311	1	1,197	0.37	0.015	0.41	468	2.13
			2	602	0.19	0.007	0.41	468	4.26
			3	511	0.16	0.006	0.41	468	6.39

Asphaltum

Test Panel Surface Destroyed by Force of Water Stream

TABLE A.7

Limited Engineering Scale Performance Test Results for Fire Nozzle on Roofing Materials  
Particle Size Range 88-177  $\mu$ ; Nominal Mass Loading 50.0 g/ft<sup>2</sup>

Surface	Average Initial Mass $\bar{M}_0$ (g/ft <sup>2</sup> )	Average Initial Radiation $\bar{I}_0$ (cpm)	Pass No.	Average Residual Radiation $\bar{I}$ (cpm)	Average Residual Mass $\bar{M}$ (g/ft <sup>2</sup> )	Average Residual Fraction $\bar{F}$	Time per Pass $\tau$ (min)	Rate of Removal $\bar{R}$ (ft <sup>2</sup> /min)	Cumulative Effort $\bar{E}$ $\left(\frac{\text{Noz Min}}{10^3 \text{ ft}^2}\right)$
Test panel surface destroyed by force of water stream									
Asphaltum									
Composition Shingle	52.02	174,230	1	9,366	2.80	0.054	0.51	376	2.66
			2	4,063	1.21	0.023	0.51	376	5.32
			3	3,416	1.02	0.020	0.51	376	7.98
Fiber-glass	49.66	165,828	1	647	0.19	0.004	0.52	369	2.71
			2	520	0.15	0.003	0.52	369	5.42
			3	408	0.12	0.0025	0.52	369	8.13
Corrugated Metal	50.25	160,826	1	1,841	0.57	0.011	0.51	376	2.66
			2	1,353	0.42	0.008	0.51	376	5.32
			3	1,245	0.39	0.008	0.51	376	7.98

TABLE A.8

Limited Engineering Scale Performance Test Results for Fire Nozzle on Roofing Materials  
Particle Size Range 88-177  $\mu$ ; Nominal Mass Loading 100.0 g/ft<sup>2</sup>

Surface	Average Initial Mass $M_0$ (g/ft <sup>2</sup> )	Average Initial Radiation $I_0$ (cpm)	Pass No.	Average Residual Radiation $I$ (cpm)	Average Residual Mass $M$ (g/ft <sup>2</sup> )	Average Residual Fraction $F$	Time per Pass $t$ (min)	Rate of Removal $R$ (ft <sup>2</sup> /min)	Cumulative Effort $\Sigma$ ( $\frac{\text{Noz Min}}{10^3 \text{ ft}^2}$ )
Test panel surface destroyed by force of water stream									
Asphaltum Composition Shingle	104.04	372,663	1	15,796	4.91	0.042	0.72	267	3.75
			2	7,684	2.14	0.021	0.72	267	7.56
			3	6,283	1.76	0.017	0.72	267	11.25
Fiber-glass	99.31	312,417	1	476	0.15	0.0015	0.78	246	4.06
			2	405	0.13	0.0013	0.71	270	7.76
			3	-	-	-	-	-	-
Corrugated Metal	98.1	355,034	1	1,948	0.54	0.005	0.72	267	3.75
			2	1,102	0.30	0.003	0.72	267	7.50
			3	1,041	0.28	0.003	0.72	267	11.25



TABLE A.9

Limited Engineering Scale Performance Test Results for Fire Nozzle on Roofing Materials  
Particle Size Range 300-600  $\mu$ ; Nominal Mass Loading 5.0 g/ft<sup>2</sup>

Surface	Average Initial Mass $M_0$ (g/ft <sup>2</sup> )	Average Initial Radiation $I_0$ (cpm)	Pass No.	Average Residual Radiation $I$ (cpm)	Average Residual Mass $M$ (g/ft <sup>2</sup> )	Average Residual Fraction $F$	Time per Pass $t$ (min)	Rate of Removal $R$ (ft <sup>2</sup> /min)	Cumulative Effort $E$ $\left(\frac{\text{Noz Min}}{10^3 \text{ ft}^2}\right)$
Asphaltum	4.73	38,106	1	107	0.02	0.003	0.37	518	1.93
			2	-	-	-	-	-	-
			3	-	-	-	-	-	-
Composition Shingle	5.91	48,981	1	6,317	0.76	0.129	0.36	533	1.87
			2	2,685	0.32	0.055	0.36	533	3.74
			3	1,923	0.23	0.039	0.36	533	5.61
Fiber-glass	5.91	33,877	1	53	0.01	0.002	0.37	518	1.93
			2	58	0.01	0.002	0.35	548	3.75
			3	-	-	-	-	-	-
Corrugated Metal	4.73	26,975	1	462	0.08	0.017	0.35	548	1.81
			2	121	0.02	0.004	0.35	548	3.68
			3	61	0.01	0.002	0.35	548	5.52

TABLE A.10

Limited Engineering Scale Performance Test Results for Fire Nozzle on Roofing Materials  
Particle Size Range 300-600  $\mu$ ; Nominal Mass Loading 25.0 g/ft<sup>2</sup>

Surface	Average Initial Mass $\bar{M}_0$ (g/ft <sup>2</sup> )	Average Initial Radiation $\bar{I}_0$ (c/m)	Pass No.	Average Residual Radiation $\bar{I}$ (c/m)	Average Residual Mass $\bar{M}$ (g/ft <sup>2</sup> )	Average Residual Fraction $\bar{F}$	Time per Pass $t$ (min)	Rate of Removal $R$ (ft <sup>2</sup> /min)	Cumulative Effort $Z$ $\left(\frac{\text{Noz Min}}{10^3 \text{ ft}^2}\right)$
Asphal- tum	23.65	175,720	1	500	0.07	0.003	0.42	457	2.19
			2	418	0.06	0.002	0.42	457	4.38
			3	-	-	-	-	-	-
Composi- tion Shingle	26.01	203,694	1	11,152	1.42	0.055	0.42	457	2.19
			2	4,626	0.59	0.023	0.42	457	4.38
			3	3,481	0.44	0.017	0.42	457	6.57
			4	3,102	0.39	0.015	0.42	457	0.76
Fiber- glass	24.83	200,431	1	173	0.02	0.001	0.42	457	2.19
			2	-	-	-	-	-	-
			3	-	-	-	-	-	-
Corruga- ted Metal	24.83	197,152	1	409	0.05	0.002	0.42	457	2.19
			2	108	0.01	0.0005	0.42	457	4.38
			3	-	-	-	-	-	-

TABLE A.11

Limited Engineering Scale Performance Test Results for Flare Nozzle on Roofing Materials  
Particle Size Range 88-177  $\mu$ ; Nominal Mass Loading 12.0 g/ft<sup>2</sup>

Surface	Average Initial Mass $\bar{M}_0$ (g/ft <sup>2</sup> )	Average Initial Radiation $\bar{I}_0$ (cpm)	Pass No.	Average Residual Radiation $\bar{I}$ (cpm)	Average Residual Mass $\bar{M}$ (g/ft <sup>2</sup> )	Average Residual Fraction $\bar{F}$	Time Per Pass $t$ (min)	Rate of Removal $R$ (ft <sup>2</sup> /min)	Cumulative Effort $E$ ( $\frac{\text{Noz Min}}{10^3 \text{ ft}^2}$ )
Asphalt-tum	9.46	15,063	1	66	0.042	0.004	0.32	600	1.67
			2	23	0.014	0.001	0.32	600	3.34
			3	16	0.010	0.001	0.32	600	5.01
Composition Shingle	11.82	22,583	1	2,547	1.333	0.113	0.32	600	1.67
			2	1,422	0.745	0.063	0.34	565	3.44
			3	1,101	0.576	0.049	0.32	600	5.11
Fiber-glass (reading high - simulant stuck to soft surface)	10.64	15,193	1	1,456	1.02	0.096	0.32	600	1.67
			2	1,503	1.05	0.099	0.32	600	3.34
			3	1,245	0.87	0.082	0.32	600	5.01
Corrugated Metal	10.64	19,903	1	83	0.04	0.004	0.32	600	1.67
			2	85	0.05	0.004	0.31	619	3.28
			3	97	0.05	0.005	0.32	600	4.95

TABLE A.12

Limited Engineering Scale Performance Test Results for Flare Nozzle on Roofing Materials  
Particle Size Range 88-177  $\mu$ ; Nominal Mass Loading 25.0 g/ft<sup>2</sup>

Surface	Average Initial Mass $\bar{M}_0$ (g/ft <sup>2</sup> )	Average Initial Radiation $\bar{I}_0$ (cpm)	Pass No.	Average Residual Radiation $\bar{I}$ (cpm)	Average Residual Mass $\bar{M}$ (g/ft <sup>2</sup> )	Average Residual Fraction $\bar{F}$	Time per Pass $t$ (min)	Rate of Removal $R$ (ft <sup>2</sup> /min)	Cumulative Effort $E$ ( $\frac{\text{Noz Min}}{10^3 \text{ ft}^2}$ )
Asphaltum	24.83	52,351	1	270	0.13	0.005	0.42	457	2.19
			2	316	0.15	0.006	0.42	457	4.38
			3	-	-	-	-	-	-
Composition Shingle	27.19	57,639	1	1,955	1.07	0.034	0.44	436	2.29
			2	1,528	0.72	0.026	0.41	468	4.42
			3	1,468	0.69	0.025	0.42	457	6.61
Fiber-glass	24.83	46,177	1	95	0.05	0.002	0.42	457	2.19
			2	76	0.04	0.002	0.42	457	4.38
			3	-	-	-	-	-	-
Corrugated Metal	23.65	44,334	1	280	0.15	0.006	0.41	468	2.13
			2	227	0.12	0.005	0.42	457	4.32
			3	-	-	-	-	-	-

TABLE A.13

Limited Engineering Scale Performance Test Results for Flare Nozzle on Roofing Materials  
Particle Size Range 88-177  $\mu$ ; Nominal Mass Loading 50.0 g/ft<sup>2</sup>

Surface	Average Initial Mass $\bar{M}_0$ (g/ft <sup>2</sup> )	Average Initial Radiation $\bar{I}_0$ (cpm)	Pass No.	Average Residual Radiation $\bar{I}$ (cpm)	Average Residual Mass $\bar{M}$ (g/ft <sup>2</sup> )	Average Residual Fraction $\bar{F}$	Time per Pass $t$ (min)	Rate of Removal $R$ (ft <sup>2</sup> /min)	Cumulative Effort $E$ $\left(\frac{\text{Noz Min}}{10^3 \text{ ft}^2}\right)$
Asphalt- turf	53.20	93,331	1	92	0.05	0.001	0.51	376	2.66
			2	100	0.06	0.001	0.50	384	5.26
			3	-	-	-	-	-	-
Composi- tion Shingle	48.47	101,952	1	1,853	0.88	0.018	0.50	384	2.60
			2	1,362	0.65	0.013	0.51	376	5.26
			3	1,170	0.56	0.011	0.51	376	7.92
Fiber- glass	50.84	96,717	1	10	0.005	0.0001	0.43	446	2.24
			2	-	-	-	-	-	-
			3	-	-	-	-	-	-
Corru- gated Metal	47.29	98,233	1	569	0.27	0.005	0.51	376	2.66
			2	353	0.17	0.004	0.51	376	5.32
			3	321	0.16	0.003	0.50	384	7.92

TABLE A.14

Limited Engineering Scale Performance Test Results for Flare Nozzle on Roofing Materials  
Particle Size Range 88-177  $\mu$ ; Nominal Mass Loading 100.0 g/ft<sup>2</sup>

Surface	Average Initial Mass $M_o$ (g/ft <sup>2</sup> )	Average Initial Radiation $\bar{I}_o$ (cpm)	Pass No.	Average Residual Radiation $\bar{I}$ (cpm)	Average Residual Mass $\bar{M}$ (g/ft <sup>2</sup> )	Average Residual Fraction $\bar{F}$	Time per Pass $t$ (min)	Rate of Removal $R$ (ft <sup>2</sup> /min)	Cumulative Effort $E$ $\left(\frac{\text{Noz Min}}{10^3 \text{ ft}^2}\right)$
Asphaltum	96.95	189,140	1	105	0.05	0.0005	0.71	270	3.70
			2	-	-	-	-	-	-
			3	-	-	-	-	-	-
Composition Shingle	96.95	188,456	1	2,950	1.51	0.016	0.70	274	3.65
			2	2,321	1.19	0.012	0.70	274	7.30
			3	2,189	1.12	0.012	0.71	270	11.00
Fiber-glass	100.49	214,047	1	29	0.01	0.0001	0.60	320	3.25
			2	-	-	-	-	-	-
			3	-	-	-	-	-	-
Corrugated Metal	108.77	210,213	1	1,186	0.61	0.006	0.67	286	3.49
			2	695	0.36	0.003	0.68	282	7.03
			3	570	0.29	0.003	0.69	278	10.62

TABLE A.15

Limited Engineering Scale Performance Test Results for Flare Nozzle on Roofing Materials  
Particle Size Range 300-600  $\mu$ ; Nominal Mass Loading 5.0 g/ft<sup>2</sup>

Surface	Average Initial Mass $M_o$ (g/ft <sup>2</sup> )	Average Initial Radiation $I_o$ (cpm)	Pass No.	Average Residual Radiation $I$ (cpm)	Average Residual Mass $M$ (g/ft <sup>2</sup> )	Average Residual Fraction $F$	Time per Pass $t$ (min)	Rate of Removal $R$ (ft <sup>2</sup> /min)	Cumulative Effort $E$ $\left(\frac{\text{Noz Min}}{10^3 \text{ ft}^2}\right)$
Asphaltum	4.73	20,916	1	55	0.01	0.003	0.32	600	1.67
			2	57	0.01	0.003	0.32	600	3.34
			3	-	-	-	-	-	-
Composition Shingle	4.73	29,338	1	1,100	0.18	0.037	0.32	600	1.67
			2	674	0.11	0.023	0.32	600	3.34
			3	594	0.09	0.020	0.32	600	5.01
Fiber-glass	4.73	35,191	1	33	0.004	0.0009	0.32	600	1.67
			2	42	0.005	0.001	0.32	600	3.34
			3	-	-	-	-	-	-
Corrugated Metal	5.91	63,753	1	236	0.02	0.004	0.32	600	1.67
			2	106	0.01	0.002	0.32	600	3.34
			3	-	-	-	-	-	-

TABLE A.16

Limited Engineering Scale Performance Test Results for Flare Nozzle on Roofing Materials  
Particle Size Range 300-600  $\mu$ ; Nominal Mass Loading 25.0 g/ft<sup>2</sup>

Surface	Average Initial Mass $M_o$ (g/ft <sup>2</sup> )	Average Initial Radiation $I_o$ (cpm)	Pass No.	Average Residual Radiation $I$ (cpm)	Average Residual Mass $M$ (g/ft <sup>2</sup> )	Average Residual Fraction $F$	Time per Pass $t$ (min)	Rate of Removal $R$ (ft <sup>2</sup> /min)	Cumulative Effort $E$ $\left(\frac{\text{Noz Min}}{10^3 \text{ ft}^2}\right)$
Asphaltum	24.83	183,514	1	183	0.02	0.001	0.42	457	2.19
			2	170	0.02	0.001	0.42	457	4.38
			3	-	-	-	-	-	-
Composition Shingle	24.83	182,442	1	1,250	0.17	0.007	0.42	457	2.19
			2	845	0.12	0.005	0.41	468	4.32
			3	708	0.10	0.004	0.41	468	6.45
Fiber-glass	24.83	181,431	1	100	0.01	0.0005	0.45	427	2.34
			2	-	-	-	-	-	-
			3	-	-	-	-	-	-
Corrugated Metal	24.83	206,886	1	327	0.04	0.002	0.42	457	2.19
			2	202	0.02	0.001	0.42	457	4.38
			3	-	-	-	-	-	-



INITIAL DISTRIBUTION

Copies

NAVY

2 Commander, Naval Ship Systems Command (SHIPS 2021)  
 1 Commander, Naval Ship Systems Command (SHIPS 03541)  
 2 Commander, Naval Facilities Engineering Command  
 1 Chief of Naval Research (Code 104)  
 1 Chief of Naval Research (Code 422)  
 1 Chief of Naval Operations (Op-75)  
 3 CO, Office of Naval Research, Branch Office, London  
 1 U. S. Naval Civil Engineering Laboratory (Library)  
 1 Director, Naval Research Laboratory  
 1 CO, Naval Training Device Center  
 1 Commandant, Marine Corps (AO3H)

ARMY

1 Director, Walter Reed Army Institute of Research (Dept. of  
 Sanitary Engineering)  
 1 Office of the Surgeon General (Redmond)  
 1 CG, Combat Developments Command, Material Requirements Div.  
 2 Army Logistics Management Center, Fort Lee (Robbins)  
 1 Ass't Secretary of the Army (R&D) (Ass't for Research)  
 3 Army Library, TAGO, Civil Defense Unit, Washington  
 1 The Engineer School, Fort Belvoir  
 1 Army Engineer Research and Development Laboratories (Tech. Lib.)  
 1 Office of the Chief of Engineers, Joint Civil Defense Support  
 Group  
 1 Army Nuclear Defense Laboratory (Technical Library)  
 1 Army Nuclear Defense Laboratory, Army Chemical Center (Maloney)  
 1 Army Map Service (Code 9001) (Vulnerability Analysis)  
 1 Medical Field Service School (Dept. Prev. Med.) (C. Lewis)  
 1 Army War College (Library)  
 1 Army Material Office, Directorate of R&D, Fort Belvoir (Schmidt)  
 1 Chief of Research and Development (Atomic Office)  
 1 Deputy Chief of Staff for Military Operations (CBR)  
 1 Hq., Dugway Proving Ground  
 1 CG, Army Electronics Command (AMSEL-BL-MA, Mr. Conover)  
 1 CO, Army Combat Developments Command, Nuclear Group (Delamain)

1 CO, Army Combat Developments Command, CBR Agency (Whitten)  
1 Office of Civil Defense, Training Program (McConnell)  
75 Office of Civil Defense (Dir. for Research)

#### AIR FORCE

1 Ass't Secretary of the Air Force (R&D)  
1 Air University, Maxwell AFB (Library)  
1 Air Force Special Weapons Center, Kirtland AFB (Library)  
1 Air Force Special Weapons Center, Kirtland AFB (WLRB)  
1 Director, USAF Project RAND

#### OTHER DOD ACTIVITIES

2 Institute for Defense Analysis (Knapp, Eastman)  
1 Advanced Research Projects Agency  
1 Defense Atomic Support Agency, Washington (Library)  
1 Commander, FC/DASA, Sandia Base  
1 Commander, FC/DASA, Sandia Base (FCTG5, Library)  
1 Defense Communications Agency, Arlington  
1 Defense Intelligence Agency (DIAAP-1K2)  
1 Chief, National Military Command System Support Center,  
Washington  
2 Office of Emergency Planning, Research Div. (Green, Coker)  
20 Defense Documentation Center

#### AEC ACTIVITIES AND OTHERS

1 American Institute for Research, Pittsburgh  
2 Atomic Energy Commission, Germantown (Reports Library, G-017,  
Deal)  
1 Atomic Energy Commission, Oak Ridge (Tech. Info. Serv.)  
1 Battelle, N. W., Richland (Larson)  
1 Brookhaven National Laboratory (Sparrow)  
1 Department of Agriculture, Agricultural Research Service  
1 Department of Agriculture, Agricultural Research (Ass't to the  
Administrator)  
1 Department of Commerce, Water and Sewage Industry and  
Utilities Division  
1 Dikewood Corporation, Albuquerque (Wood)  
1 Engineering Science, Inc., Arcadia (Ludwig)  
1 Ford Instrument Company, Long Island City (Polan)  
1 Geological Survey, Water Resources Division  
1 Hudson Institute (Kahn)  
1 IIT Research Institute (Sevin)  
1 Ionics, Incorporated, Cambridge (McRae)

1 Lawrence Radiation Laboratory, Livermore (Shore)  
 1 Merrimack College, North Andover (Grune)  
 1 Hq., NASA, Office of Advanced Research and Technology  
 1 National Academy of Sciences (Park)  
 3 Oak Ridge National Laboratory (Auerbach, Wigner, Parker)  
 1 Office of Education, Dir., Civil Def. Adult Education Staff  
 1 PARM Project  
 1 Public Health Service, Washington (Parrino)  
 1 Public Health Service, Washington (DHEW, Terrell)  
 1 Public Health Service, Las Vegas (Seal)  
 1 RAND Corporation (Mitchell)  
 2 Research Triangle Institute (Parsons, Ryan)  
 4 Stanford Research Institute (White, Miller)  
 1 Technical Operations Research (Clarke)  
 1 University of California, Davis (Bustad)  
 1 URS Corporation (Hawkins)  
 15 Division of Technical Information Extension, Oak Ridge

USNRDL

45 Technical Information Division

DISTRIBUTION DATE: 18 October 1966

DOCUMENT CONTROL DATA - R&D		
(Security classification of title, body of abstract and indexing annotation must be entered when the overall report is classified)		
1. ORIGINATING ACTIVITY (Corporate author) U. S. Naval Radiological Defense Laboratory San Francisco, California 94135		2a. REPORT SECURITY CLASSIFICATION UNCLASSIFIED
		2b. GROUP
3. REPORT TITLE  THREE TESTS OF FIREHOSING TECHNIQUE AND EQUIPMENT FOR THE REMOVAL OF FALLOUT FROM ASPHALT STREETS AND ROOFING MATERIALS		
4. DESCRIPTIVE NOTES (Type of report and inclusive dates)		
5. AUTHOR(S) (Last name, first name, initial)  Wiltshire, Lyman L. Owen, W. Leigh		
6. REPORT DATE 18 October 1966	7a. TOTAL NO. OF PAGES 74	7b. NO. OF PAGES 9
8a. CONTRACT OR GRANT NO.	9a. ORIGINATOR'S REPORT NUMBER(S) USNRDL-TR-1048	
b. PROJECT NO.		
c. OCD-TO-65-200(22), Work Unit 3212A	9b. OTHER REPORT NO(S) (Any other numbers that may be assigned this report)	
d.		
10. AVAILABILITY/LIMITATION NOTICES  Distribution of this document is unlimited.		
11. SUPPLEMENTARY NOTES	12. SPONSORING MILITARY ACTIVITY Office of Civil Defense Washington, D.C. 20310	
13. ABSTRACT This report describes three separate firehosing experiments. Each employed radio-traced simulant in order to measure removal effectiveness. Two of the experiments, which were conducted on asphalt streets, concluded the test series started in 1963. The first experiment investigated the feasibility of the NRDL flare nozzle as a reclamation tool for paved surfaces. The second experiment consisted of the full scale reclamation of a street area. This provided operational data and firehose-crew exposure-rate histories. The third experiment, which involved the reclamation of roof surfaces, was a renewal of earlier work performed by this laboratory between 1952 and 1958. New roofing materials were tried and particle size effects were measured. From these three experiments it was concluded that: 1. Effectiveness of reclamation by firehosing improves as surface roughness decreases and particle size increases. 2. Removal effectiveness improves with effort, but the residual mass is not significantly reduced after the second pass. 3. The flare nozzle is consistently more effective than the fire nozzle in cleaning roof surfaces. This is not the case for paved surfaces. 4. Results from full scale tests show that the removal effectiveness can never equal that achieved under the less realistic operating conditions represented by smaller engineering-scale tests. 5. $RN_{50}$ exposure reduction factors are not significantly affected by surface roughness, particle size or mass loading.		

UNCLASSIFIED

Security Classification

14.

## KEY WORDS

Reclamation  
 Firehosing effectiveness  
 Surface roughness  
 Residual number (RN<sub>2</sub>) values  
 Firehose stream pattern  
 Fallout mass loading  
 Particle size

## LINK A

## LINK B

## LINK C

ROLE

WT

ROLE

WT

ROLE

WT

## INSTRUCTIONS

1. **ORIGINATING ACTIVITY:** Enter the name and address of the contractor, subcontractor, grantee, Department of Defense activity or other organization (corporate author) issuing the report.

2a. **REPORT SECURITY CLASSIFICATION:** Enter the overall security classification of the report. Indicate whether "Restricted Data" is included. Marking is to be in accordance with appropriate security regulations.

2b. **GROUP:** Automatic downgrading is specified in DoD Directive 5200.10 and Armed Forces Industrial Manual. Enter the group number. Also, when applicable, show that optional markings have been used for Group 3 and Group 4 as authorized.

3. **REPORT TITLE:** Enter the complete report title in all capital letters. Titles in all cases should be unclassified. If a non-classified title cannot be selected without classification, show title classification in all capitals in parenthesis immediately following the title.

4. **DESCRIPTIVE NOTES:** If appropriate, enter the type of report, e.g., interim, progress, summary, annual, or final. Give the inclusive dates when a specific reporting period is covered.

5. **AUTHOR(S):** Enter the name(s) of author(s) as shown on or in the report. Enter last name, first name, middle initial. If military, show rank and branch of service. The name of the principal author is an absolute minimum requirement.

6. **REPORT DATE:** Enter the date of the report as day, month, year, or month, year. If more than one date appears on the report, use date of publication.

7a. **TOTAL NUMBER OF PAGES:** The total page count should follow normal pagination procedures, i.e., enter the number of pages containing information.

7b. **NUMBER OF REFERENCES:** Enter the total number of references cited in the report.

8a. **CONTRACT OR GRANT NUMBER:** If appropriate, enter the applicable number of the contract or grant under which the report was written.

8b, 8c, & 8d. **PROJECT NUMBER:** Enter the appropriate military department identification, such as project number, subproject number, system numbers, task number, etc.

9a. **ORIGINATOR'S REPORT NUMBER(S):** Enter the official report number by which the document will be identified and controlled by the originating activity. This number must be unique to this report.

9b. **OTHER REPORT NUMBER(S):** If the report has been assigned any other report numbers (either by the originator or by the sponsor), also enter this number(s).

10. **AVAILABILITY/LIMITATION NOTICES:** Enter any limitations on further dissemination of the report, other than those

imposed by security classification, using standard statements such as:

- (1) "Qualified requesters may obtain copies of this report from DDC."
- (2) "Foreign announcement and dissemination of this report by DDC is not authorized."
- (3) "U. S. Government agencies may obtain copies of this report directly from DDC. Other qualified DDC users shall request through \_\_\_\_\_."
- (4) "U. S. military agencies may obtain copies of this report directly from DDC. Other qualified users shall request through \_\_\_\_\_."
- (5) "All distribution of this report is controlled. Qualified DDC users shall request through \_\_\_\_\_."

If the report has been furnished to the Office of Technical Services, Department of Commerce, for sale to the public, indicate this fact and enter the price, if known.

11. **SUPPLEMENTARY NOTES:** Use for additional explanatory notes.

12. **SPONSORING MILITARY ACTIVITY:** Enter the name of the departmental project office or laboratory sponsoring (paying for) the research and development. Include address.

13. **ABSTRACT:** Enter an abstract giving a brief and factual summary of the document indicative of the report, even though it may also appear elsewhere in the body of the technical report. If additional space is required, a continuation sheet shall be attached.

It is highly desirable that the abstract of classified reports be unclassified. Each paragraph of the abstract shall end with an indication of the military security classification of the information in the paragraph, represented as (TS), (S), (C), or (U).

There is no limitation on the length of the abstract. However, the suggested length is from 150 to 225 words.

14. **KEY WORDS:** Key words are technically meaningful terms or short phrases that characterize a report and may be used as index entries for cataloging the report. Key words must be selected so that no security classification is required. Identifiers, such as equipment model designation, trade name, military project code name, geographic location, may be used as key words but will be followed by an indication of technical context. The assignment of links, roles, and weights is optional.